RESEARCH ARTICLE
doi:10.59236/geomorphica.v2i1.44

GEOMORPHICA

On the attraction of marine dunes to OWF fixed foundations

Noémie Durand * [1,3], **Pablo Tassi** [2,3], **Olivier Blanpain** [1], **Alice Lefebvre** [4]

[1]France Energies Marines, Plouzané, France, [2]EDF Recherche & Développement, Chatou, France, [3]LHSV, Ecole des Ponts, EDF R&D, Chatou, France, [4]MARUM, University of Bremen, Germany

Author contributions: *Conceptualization*: Noémie Durand. *Methodology*: Noémie Durand. *Software*: Noémie Durand. *Formal Analysis*: Noémie Durand. *Investigation*: Noémie Durand. *Writing - original draft*: Noémie Durand. *Writing - Review & Editing*: Pablo Tassi, Alice Lefebvre. *Visualization*: Noémie Durand. *Supervision*: Pablo Tassi, Olivier Blanpain, Alice Lefebvre. *Project administration*: Alice Lefebvre. *Funding acquisition*: Pablo Tassi, Olivier Blanpain, Alice Lefebvre.

Abstract Marine dunes, also known as sand waves, are found worldwide, particularly in shallow shelf seas where marine renewable energy projects are often located. Due to their size and mobility, it is crucial for such projects to simulate dune migration and understand interactions with wind turbine foundations. This study builds upon a validated large-scale openTELEMAC model of the Dunkirk coastal area, which combines 3D hydrodynamics with a depth-averaged sediment transport approach. To evaluate the influence of wind turbine fixed foundations on dune migration, we conducted two-year numerical experiments under two contrasting scenarios: with and without foundations, thereby enabling a direct comparison with the natural baseline. The results indicate that the monopiles act as morphodynamic magnets, altering dune propagation with changes of up to a factor of 4 in their lee. We call the underlying mechanism the 'wake effect', where reduced flow velocity and sediment transport down-current of the monopile lead to increased migration rates when dunes approach the foundation and decreased (or reversed) rates when moving away. The results also highlight the cumulative effect of monopiles on sediment transport in a scenario with 46 wind turbines, emphasising the need for careful turbine placement to mitigate impacts on the dune field.

Non-technical summary Marine dunes are found all over the world, notably in shallow shelf seas where marine renewable energy projects are often located. These dunes are large, highly mobile sedimentary bedforms, typically ranging from 1 to 5 metres in height, travelling tens of metres per year. Simulating their migration over time is therefore crucial for these renewable energy projects. To assess the impact of a planned 600 MW wind farm on annual marine dune migration off Dunkirk, France, we applied the large-scale computer model of the area developed in previous work. By comparing simulations with and without the fixed foundations of the wind turbines, we evaluated how they alter the natural movement of the dunes. The results indicate that the monopiles act as sediment magnets, altering dune propagation with changes of up to a factor of 4 in their lee. Consequently, sections of the dunes move closer to the fixed foundations. The results also highlight the cumulative effect of monopiles on sediment transport in a scenario with 46 wind turbines, emphasising the need for careful turbine placement to mitigate impacts on the dune field.

Received:
November 05, 2024
Accepted:
December 02, 2025
Published:
February 26, 2026

1 Introduction

The hydrodynamics of the coastal zone is driven by tides, winds, and waves. Under their action, the seabed can be mobilised to form what is collectively known as 'bedforms'. A variety of bedforms have been observed in nature. In sandy marine environments, these include sand ripples, marine dunes, and sandbanks (see Table 1 in Knaapen, 2005, for a classification overview). Consistent with the terminology established by the Society for Sedimentary Geology (Ashley, 1990), marine dunes are large, flow-transverse bedforms typically ranging from 1 to 5 metres in height, with wavelengths on the order of hundreds of metres. In the literature, they are sometimes referred to as sand waves.

Marine dunes are highly mobile sedimentary structures, with documented migration rates of up to tens of metres per year (e.g., Bartholdy et al., 2002; Katoh et al., 1998; Le Bot et al., 2023). This constant remodelling of the seabed is a defining characteristic of marine dunes. They are frequently observed on the bed of shallow shelf seas where offshore wind farms (OWFs) are, or will be, situated. By the end of 2020, approximately 5,400 offshore wind turbines had been installed or were under construction in European waters alone (The Crown Estate, 2020). This figure is expected to increase over the coming decades to help achieve ambitious climate neutrality targets.

Therefore, more research is needed to understand how wind turbine foundations interact with their surroundings, as this topic has not been extensively explored yet. The industry has a legitimate interest in studying scour processes (van der Tempel et al., 2004; Wang et al., 2024; Whitehouse et al., 2011), which have the potential to weaken the structural integrity of the foundations. Little is known about the effects beyond the immediate vicinity (e.g., on sediment dynamics and

*Corresponding author: noedurand@openbook.team

seabed mobility), which are often dismissed as localised (e.g., Cooper and Beiboer, 2002; Clark et al., 2014). The oil and gas industry has dealt with seabed scouring around platforms or free spanning of pipelines, for example, in recent decades. However, the offshore wind industry faces two unique challenges: first, the large number of man-made structures in an OWF makes it more difficult to avoid problematic areas altogether, in contrast to a single oil platform; second, electric cables are less robust than pipelines, rendering them more vulnerable to overburden and damage (Games and Gordon, 2014).

To our knowledge, no previous studies in the literature have systematically investigated the interaction between immobile structures, such as OWF monopiles, and a dune field in a marine setting at space and time scales of the order of kilometres and months, respectively. Here, monopiles refer to large cylindrical piles driven into the seabed that extend above sea level to support offshore wind turbines. The closest relevant work is the study by Couldrey et al. (2020), which used recurrent multi-beam bathymetric surveys to document the progression of an isolated crescent-shaped dune as it migrated past an offshore wind turbine foundation. The surveys spanned six years, with one survey conducted before the installation of the monopile. Post-installation surveys focused on the cable route and wind turbine foundation, thus not covering the full extent of the dune. However, the authors noted that the dune was temporarily elongated as it passed the monopile. This stretching was partly due to natural causes, likely changes in hydrodynamics, which also affected other nearby bedforms. It was also attributed to increased sediment transport rates resulting from erosion at the dune toe and subsequent deposition a short distance downstream in the monopile wake, as the dune interacted with the scour hole at the base of the structure. This process is in accordance with the findings of Chiew (1984) and Hong et al. (2017). The authors concluded that there was no lasting impact on the dune morphology, based on the observation that transects taken 25 m on either side of the centre line are comparable pre-installation and 3 years post-installation.

Using numerical simulations, Margalit (2017) examined the formation of natural bedforms and evaluated the impact of offshore wind farms on seabed morphology. Although most of his research focused on sandbanks, one simulation considered a monopile installed within a linear marine dune field (comprising dunes measuring 3 m in height and 300 m in length). The migration rate of the dunes was said to slow as a result of the presence of the monopile. The author himself acknowledged that this simulation was exploratory. Notably, the bed elevation at the upstream boundary appears invariant, and sediment accumulates from there to the monopile without passing beyond it, raising questions about the model setup. Nevertheless, this work has the merit of initiating a discussion about the influence of monopiles on their environment.

To address the lack of systematic studies on dune-monopile interactions at kilometre-scale and multi-year temporal scales, the complex process-based model of the Dunkirk area from Durand et al. (2025) was applied to simulate these interactions in the Southern Bight of the North Sea (Figure 1), where large marine dunes are present. The model couples 3D hydrodynamics with depth-averaged sediment transport and has been shown to be capable of simulating the annual migration rates of these dunes (Durand et al., 2025). The aim of the current work is to explore the impact of the foundations of offshore wind turbines on the migration patterns. In the next section, we present the study area in the Southern Bight of the North Sea, the model setup, and validation. Initial simulations are carried out with a single monopile and then extended to a realistic OWF layout, consisting of an array of 46 wind turbines. The results of these simulations are presented in Section 3, with implications discussed in Section 4. Section 5 concludes this work.

2 Materials and methods

2.1 Study area

Dunkirk, situated in the Southern Bight of the North Sea near the French-Belgian border (Figure 1), was selected as a suitable site for an offshore wind project during France's third call for tenders in 2016. The location benefits from excellent resources, with average wind speeds between 9 and 9.5 m/s at elevations of 100 to 140 m above sea level, favourable water depths shallower than 30 m up to 20 km from the coast, and access to a robust electricity grid that is capable of handling the OWF output (Parc éolien en mer de Dunkerque website). Furthermore, Dunkirk is home to a prominent industrial port complex: the Grand Port Maritime de Dunkerque. With construction works anticipated to start in late 2026, the offshore wind farm is projected to be operational by early 2029.

A comprehensive metocean data set has been collected to support the Dunkirk OWF project and for research purposes. Site-specific meteorological and hydrodynamic campaigns have been conducted for up to six months (open-access data: Shom, 2017a) (proprietary data: FEM, 2021a; EMD, 2022). In addition, long-term metocean observations are publicly available from the Flanders Marine Institute (VLIZ) at the Westhinder measurement station (VLIZ, 2022a,b). These records provide information on wind velocity, atmospheric pressure, water level, current and wave conditions.

The region is characterised by a macro-tidal regime, with a spring tidal range equal to 5.5 m. The tide rises faster than it falls, an asymmetry that is also reflected in the tidal currents. The flood current is generally stronger than the ebb, resulting in a net current trending east-northeast. In the navigation channel (FEM, 2021a, Figure 1b), for example, peak depth-averaged speeds reach 1.22 m/s during the flood compared to 0.85 m/s during the ebb. This predominance is reversed in the gullies between the offshore sandbanks (FEM, 2021a). The near-bed currents (approximately 1 m above the bed) can reach 0.70 m/s at the peak. The offshore wind and wave climate is charac-

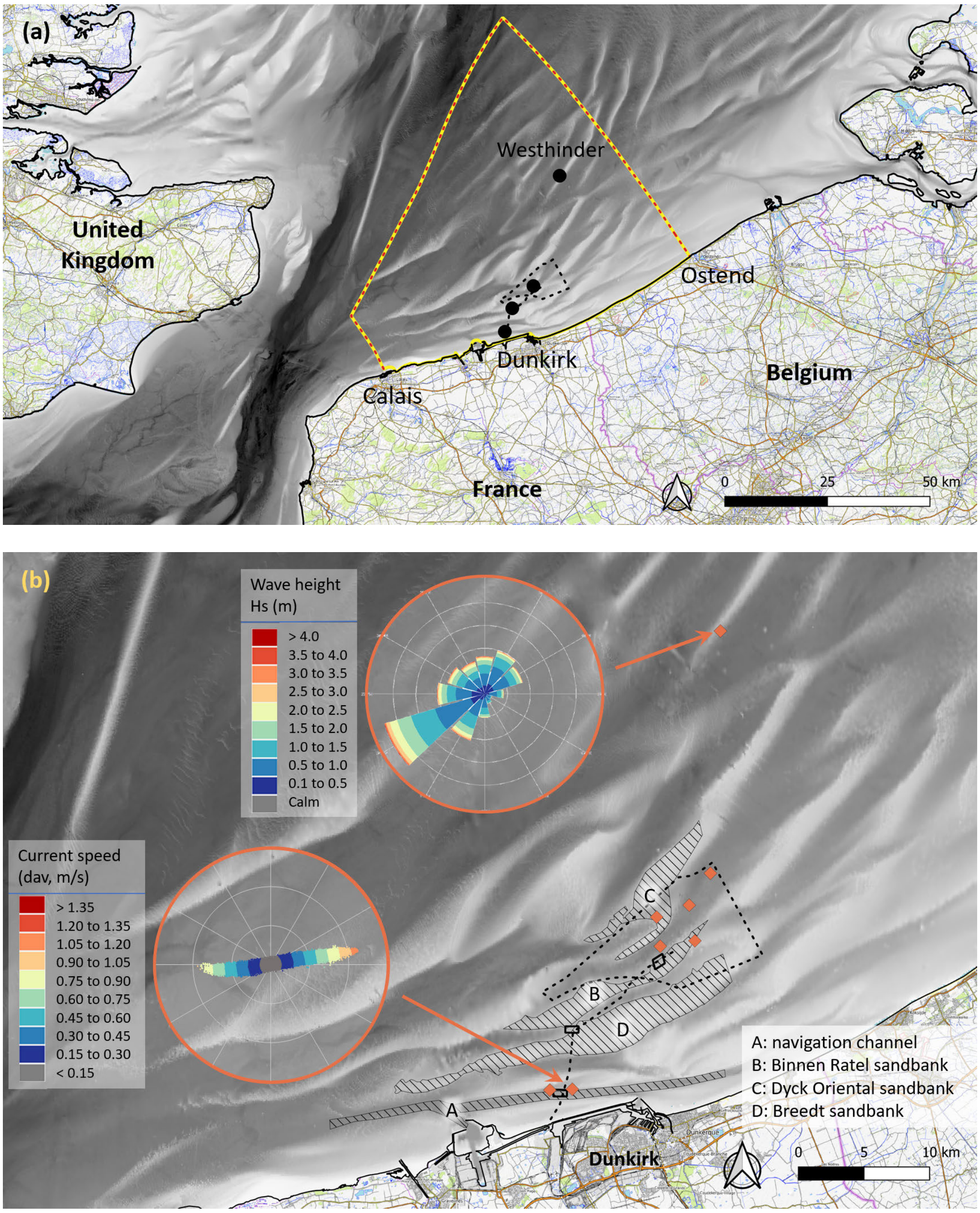

Figure 1 (**a**) General location map. The footprint of the proposed offshore wind farm is marked by a dashed black line; the extent of the numerical model by a dashed coloured line. (**b**) Location of metocean (filled diamonds) and bathymetric (polygons) survey data in relation to known bathymetric features, with accompanying rose diagrams for wave height and depth-averaged (dav) current speed climates. Source of the background data: Shom (2015), OpenTopoMap, and European Environment Agency (EEA) coastline, version 3.0.

terised by the prevalence of south-westerly events from the English Channel. However, significant events also occur from the northwest to the northeast, originating from the North Sea (Figure 1b). The wave condition with a return period of 1 year is estimated to have a significant wave height (H_s) of 4.4 m and a mean period (T_z) of approximately 7 s, as determined by an extreme value analysis of data from VLIZ (2022a). It is noteworthy that 56% of the waves are less than 1 m high.

The seabed consists primarily of non-cohesive sand with median grain sizes (d_{50}) ranging from 240 μm to 450 μm and d_{10} averaging 210 μm (FEM, 2020). These sediment properties favour the development of marine dunes, as confirmed by high-resolution (0.5 m) bathymetric surveys conducted between 2016 and 2021. Two full-coverage surveys mapped the wind farm footprint (black dashed outline in Figure 1): an open-access campaign from 2016–2017 (Shom, 2017b) and a proprietary survey in June 2021 (EMD, 2021). Eight additional surveys were performed between 2019 and 2021 in three representative areas, capturing diverse bedform features at the same 0.5 m resolution (FEM, 2021b, black circles/polygons in Figure 1).

These surveys reveal marine dunes with heights of between 1 and 4 m (7–20% of the local water depth) and wavelengths of 150–200 m. The dunes display distinct morphological patterns across the study area. The majority are sharp-crested and strongly asymmetrical, with a gentler side and a steeper side, reflecting a dominant current direction (Figure 2). This asymmetry systematically decreases towards sandbank crests, where dunes transition to symmetrical forms, reflecting reworking during both flood and ebb tides. Notably, dune fields are well-developed on sandbank crests and flanks

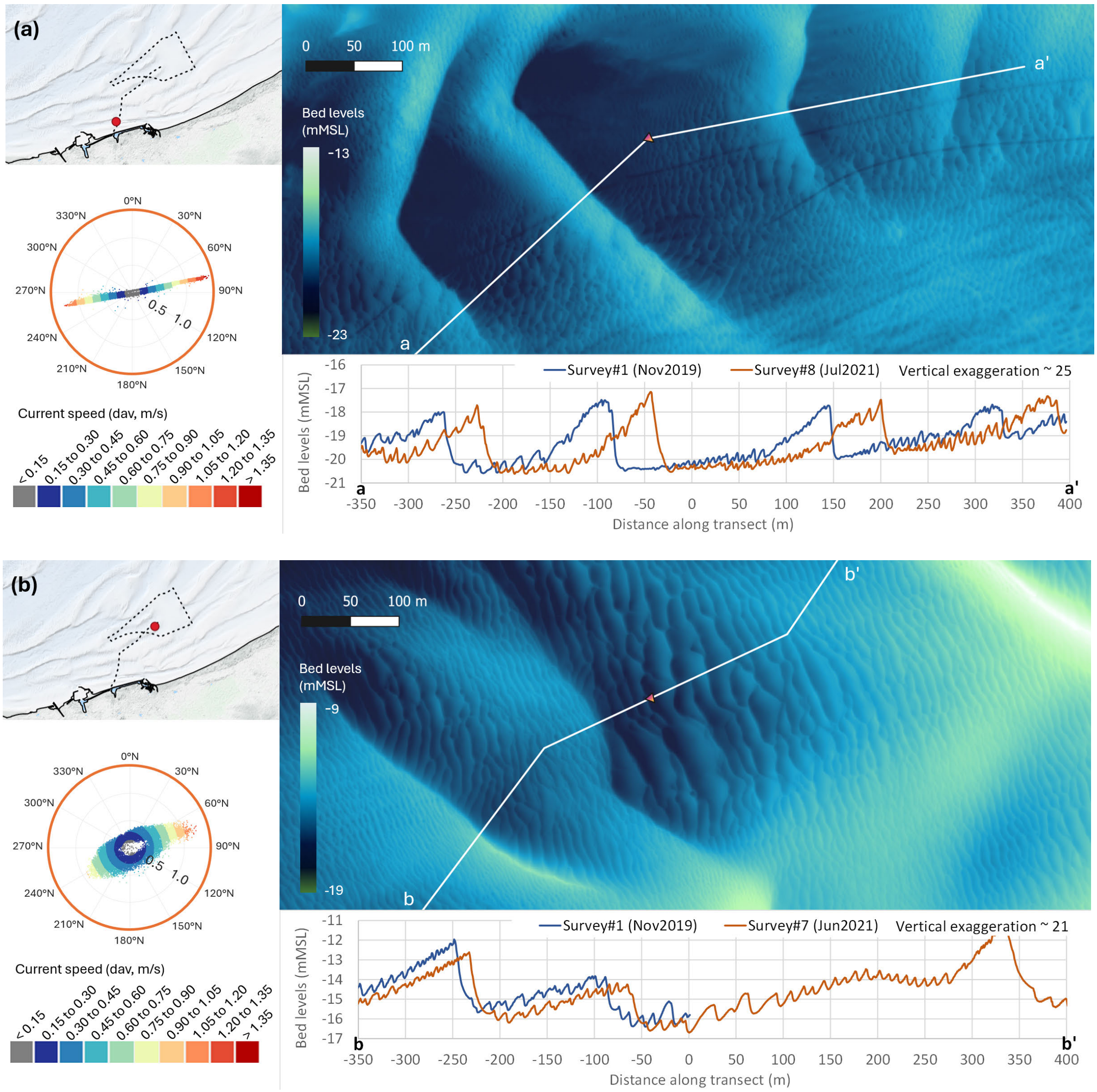

Figure 2 For Case IA (**a**) and Case IB (**b**): Location of the monopile, indicated by a coloured triangle, to scale, relative to the OWF project and local dune field, with cross-dune seabed profiles (November 2019 vs. June/July 2021). Current ellipses characterise the local depth-averaged (dav) hydrodynamic conditions.

(e.g., sinuous dunes with frequent bifurcations dominate the flanks of the Dyck Oriental sandbank) but become sparse or absent in the deeper gullies between banks. The repeated surveys have allowed the annual dune migration rate to be quantified (Le Bot et al., 2023). Overall, they have been observed to travel at a net rate of approximately 30 m/yr towards the northeast.

2.2 Model set-up and pre-construction validation

This study builds upon the open**TELEMAC** model of the Dunkirk coastal area, which was originally developed to investigate meteorological controls on a marine dune field (Durand et al., 2025). The computational domain extends from Calais to Ostend in Belgium, covering approximately 80 km of coastline. Its offshore extent varies between 15 km in the Dover Strait and 75 km in the east (dashed coloured line in Figure 1a). An unstructured finite element mesh with spatially varying resolution is used. The size of the triangular elements varies gradually from 10 m (covering between 2.5 km^2 and 44 km^2 around offshore wind turbine infrastructure, providing 10–20 grid points per dune wavelength) to a maximum of 3000 m in distant areas, ensuring both adequate resolution of the dunes where interactions with structures are of interest and computational efficiency. Digital terrain models (DTMs) of the seabed throughout the computational domain have been constructed from a range of data sources, with the most recent and detailed data given precedence over data of lesser quality.

The hydrodynamic module, TELEMAC-3D, is coupled with the sediment transport and bed evolution module, GAIA, to consider the interactions between tidal flows, weather and sediment transport processes. The influence of waves is omitted in this model since Durand et al. (2023a) suggested that waves are of secondary importance in waters deeper than approximately 15 m be-

Table 1 Modelling parameters and processes used in open**TELEMAC** (TELEMAC-3D+GAIA modules)

Vertical discretisation	3D with 5 irregularly spaced sigma planes
Horizontal discretisation	At least 10 grid points per dune wavelength
Bathymetric data sources	0.5–1 m resolution: EMD (2021); FEM (2021b); Shom (2017b); Shom - ROLNHDF (2022) 20–100 m resolution: Shom (2015, 2016); Flemish Hydrography (2022)
Tidal constituents	34 harmonic constituents at 1/16 resolution (FES2014; Lyard et al., 2021)
Wind & sea level pressure	Hourly data at 1/40 resolution (AROME 30-hour forecast; Bouttier, 2007)
Friction	Nikuradse roughness $k_s = 2.5 \times d_{50}$ (Soulsby, 1997)
Horizontal turbulent diffusion	Constant kinematic viscosity = 10^6 m^2/s
Vertical turbulent diffusion	Tsanis mixing length model (Tsanis, 1989)
Dynamic pressure	Yes
Hydrodynamic model performance	Relative Mean Absolute Error (MAE) < 3% for water levels and < 18% for currents
Sediment type	One class of non-cohesive sediment; d_{50} = 345 μm (FEM, 2020)
Transport mechanism	Bedload; suspended load discarded ($P > 5$; Durand et al., 2023a)
Sediment transport predictor	Soulsby-van Rijn total load predictor (Soulsby, 1997)
Slope correction	No (Durand et al., 2023b)
Morphological factor	No
Morphodynamic model performance	Root Mean Square Error (RMSE) < 0.34 m, Anomaly Correlation Coefficient (ACC) > 84%

low mean sea level (mMSL), which is mostly the case in our areas of interest. TELEMAC-3D solves the 3D Reynolds-Averaged Navier-Stokes equations without a hydrostatic pressure assumption (Hervouet, 2007, see Supplementary Materials). The hydrodynamics were calibrated and validated by comparing the model predictions with site-specific water level and current data at 7 locations across the computational domain (EMD, 2022; FEM, 2021a; Shom, 2017a; VLIZ, 2022b), achieving 'excellent' performance according to the Sutherland et al. (2004) classification scheme (see Table 1 for key metrics).

GAIA solves the sediment continuity equation (Exner equation) to compute the seabed evolution from empirical sediment transport rate predictors (Tassi et al., 2023, see Supplementary Materials). A single, representative sediment class (d_{50} = 345 μm) was adopted, reflecting the in situ surficial bed samples that showed a dominant unimodal distribution without spatial or seasonal trends. For this grain size, shear velocities during peak flows ($u_* \sim$ 3.9 cm/s) remain below the settling velocity ($w_s \sim$ 4.4 cm/s; Soulsby, 1997). A Rouse parameter analysis ($P > 5$; Durand et al., 2023a) further confirms bedload dominance in the area. These findings, consistent with the presence of marine dunes, justify excluding suspended load from the model. In keeping with the model developed in Durand et al. (2025), the Soulsby-van Rijn predictor (Soulsby, 1997) was used, without slope correction, which was found to cause unrealistic dune decay (Durand et al., 2023b). This choice was based on preliminary tests showing it to be as effective as other shear-stress-based formalisms at reproducing annual dune migration. Although a depth-averaged approach, its energy-based formulation scales bedload transport rates with flow kinetic energy, inherently capturing transport maxima over dune crests and enabling realistic migration without resolving near-bed flow. A scaling factor was applied in the original application, which successfully reproduced observed dune migration patterns (FEM, 2021b), thereby validating the model (Durand et al., 2025, Table 1 for metrics).

2.3 Simulated scenarios and analysis of results

To assess the impact of turbine foundations on the evolution of large marine dunes, we have simulated a two-year period. A baseline simulation was initially performed to model the hydrodynamic and sediment transport processes naturally occurring offshore Dunkirk, without any monopiles influencing them. We then adopted a sequential modelling strategy, beginning with exploratory single-monopile scenarios in well-characterised, data-rich environments where baseline morphodynamics were validated, before progressing to realistic full-array simulations of the actual Dunkirk OWF layout. This sequential methodology allowed us to analyse foundation effects across scales, from isolated to array-wide interactions.

In all cases, we remove the triangular mesh elements corresponding to each monopile location, specifically one element per foundation, where the effective obstruction is determined by the horizontal resolution of the mesh. This approach is more practical and efficient to implement than the alternative of parameterising the monopiles as additional drag, which requires estimating the undisturbed upstream flow. It accurately captures their physical role as full water-column obstructions by creating a vertical null-flux boundary (through

Table 2 Characteristics of monopiles in the exploratory and OWF scenarios.

Scenario		Number monopiles	Position (Latitude,Longitude)	Water depth (mMSL)	Average edge length† (m)
Exploratory:	Case IA	1	(5103.830'N, 215.801'E)	-20.1	10.7
	Case IB	1	(5109.239'N, 222.644'E)	-15.6	10.3
OWF:	Case II*	46	–	-10.6 to -28.8	9.0 to 14.7 (10.6)
	Case IIA*	24	–	-10.6 to -28.4	9.6 to 12.5 (10.8)
	Case IIB	22	–	-10.9 to -28.8	9.0 to 14.7 (10.5)

† Monopile diameters ranging from 7.0 m to 11.5 m are planned for the Dunkirk OWF

* Excluding 2 monopiles placed at the edge of the refined zone (outside the dune field)

element removal) that enforces free-slip flow conditions and zero sediment flux across all depths. This implementation choice aligns with Rivier et al. (2015, 2016), who used a 3D hydrodynamic and sediment transport model to explore potential differences arising from monopile representations (either a resistance term in the momentum equation and a source term in the turbulence equation, or mesh-resolved structures) and observed minimal impact on near-field flow velocities.

Since the wind farm is not yet constructed, no field data exist for flow conditions with turbine foundations at our study site, preventing a full calibration of the hydrodynamics with monopiles. Nevertheless, confidence in the model adaptation is supported by a realistic prediction of the monopile hydrodynamic wake (see Supplementary Materials, Figures S1-S2). The results show an elongated wake structure consistent with the bidirectional tidal currents. This wake decays over a spatially consistent scale, with surface velocity recovering to 80% within approximately 900 m downstream and reaching 95% recovery by 2.0 km. This recovery length aligns with observational findings from the Donghai Bridge offshore wind farm (Li et al., 2014) and numerical simulations of the planned Courseulles farm (Rivier et al., 2016). Furthermore, the model captures an expected dependency on the flow incidence angle relative to the removed triangular mesh element. This dependency is seen not in the overall length of the wake, but in the rate of velocity recovery and the detailed structure of the near-wake region.

2.3.1 Exploratory scenarios

To investigate the fundamental interactions between annual marine dune migration and a fixed foundation, we developed hypothetical scenarios with only one monopile as a first step; a later step will consider the impact of an OWF array as a whole. We selected the repeat survey areas, in the Dunkirk Port navigation channel and near the proposed transformer station (Figure 1), for these exploratory simulations because their well-documented bed evolution provides validated baseline conditions for natural dune evolution under hydro-meteorological forcing (Durand et al., 2025). Notably, no foundations are planned in these areas under the actual OWF layout.

In Case IA, we placed a monopile approximately 90 m ahead of the second large crescent-shaped dune (3 m high) in the navigation channel, ensuring a sufficient distance to avoid initial disturbance to the dune, and before the following sinuous dune. In Case IB, we placed a monopile on the slope on the Binnen Ratel sandbank, ca. 50 m ahead of an approaching 2 m high sinuous dune. There, the seabed topography does not constrain the flow as is the case for Case IA, leading to a broader range of directions (Figure 2).

These two cases are complementary and illustrate the range of possibilities. The first location (Case IA) is representative of a monopile sited in a gully between sandbanks, subjected to bidirectional flows that switch direction with the tidal phase, hence bidirectional sediment transport pathways. The second location (Case IB) is representative of a monopile installed on the slopes of a sandbank, in open conditions with a wider spread of directions. Table 2 and Figure 2 summarise the monopile positions and characteristics for both cases.

2.3.2 OWF scenario

Following these initial scenarios, we modelled the entire array of 46 monopiles projected for Dunkirk OWF first scenario. The foundations will support wind turbines with 220 m rotor diameters, while the monopiles themselves are expected to have 7–11.5 m diameters. The array spacing will maintain a minimum of 1 km between monopiles and 10 km from the coastline, covering an area close to 50 km^2 (Parc éolien en mer de Dunkerque website). The precise location of the monopiles was not available at the time of our work and we georeferenced the map for the 'OWF project off Dunkirk and its electrical connection' published on http://parc-eolien-en-mer-dunkerque.geophom.info/ (last updated on March 17, 2022) to extract approximate locations. Figure 3a shows this layout, including the marine dunes identified in preliminary site studies (Shom, 2017d) to provide some context. It is clear that dunes are not uniformly distributed throughout the OWF footprint. They are predominantly associated with the sandbanks, with relatively fewer dunes in the gullies between them.

We applied the same approach to represent monopiles as in exploratory scenarios, where certain elements were removed from the computational domain to define obstructions. For this simulation, the mesh was uniformly refined to a horizontal resolution of 10 m in the OWF area, covering approximately 44 km^2 (the baseline was rerun with this updated mesh discretisation for consistency). The exact size of the

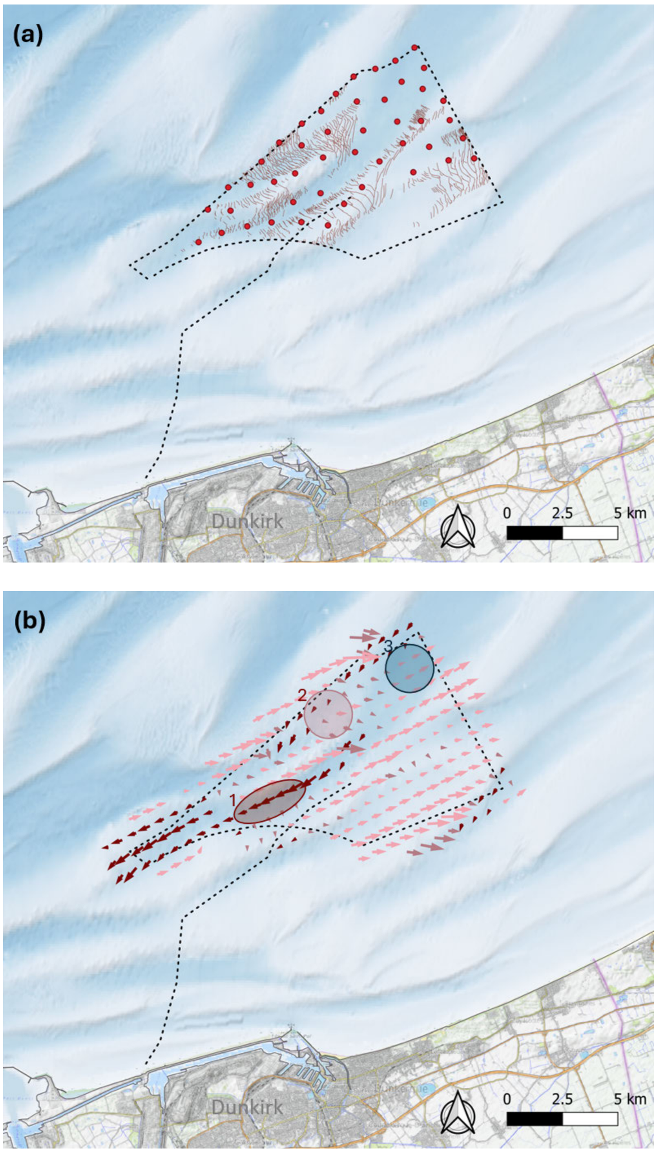

Figure 3 (**a**) One of the proposed layouts for the Dunkirk OWF; the geographical footprint and cable corridor are indicated by dashed black lines; marine dunes inventoried in Shom (2017d) are represented by sinuous brown lines. (**b**) Predicted sediment transport pathways for the baseline simulation, coloured by directional quadrant, also highlighting 3 zones of interest. Source of the background data: Shom (2015), OpenTopoMap, and European Environment Agency (EEA) coastline, version 3.0.

triangular elements varies, which in turn affects the size of the monopiles between different locations, as detailed in Table 2.

To specifically assess the influence of turbine placement, we also simulated an array comprising only half the number of wind turbines (Cases IIA and IIB). In these scenarios, turbine locations were selected to ensure that their individual effects remained spatially distinct, avoiding any a priori overlap.

The wind farm is located within a sandbank system where the prevalence of flood and ebb flows varies spatially, also influenced by meteorological conditions. As a result, sediment transport patterns and dune mobility vary spatially, as illustrated in Figure 3b. We focus our analysis on 3 morphological behaviour zones: 1) in the gully between the Binnen Ratel and the Dyck Oriental sandbanks, where the marine dunes travel towards the southwest, contrary to the general trend, 2) on the slopes of the Dyck Oriental sandbank, and 3) in a relatively flat and featureless area situated in the northern corner. These zones are indicated in Figure 3b.

2.3.3 Assessment of monopile influence

The presence of a wind turbine impacts the surrounding environment in various ways. Above sea level, it creates an atmospheric wake, which refers to a reduction in wind speed downstream of the blades. Although this can influence hydrodynamic conditions, it is usually not considered in morphodynamic modelling. Below sea level, the turbine foundation obstructs the flow, causing a downstream reduction in current speeds, known as the hydrodynamic wake. Additionally, turbulent wakes, such as horseshoe vortices near the seabed immediately upstream of the monopile and downstream vortex shedding, are generated. At the seabed level, the presence of the foundation alters the seabed morphology, with areas of erosion and accretion. This morphodynamic wake is linked to the hydrodynamic wake, as sediment transport processes respond to the changes in hydrodynamics caused by the monopile. Throughout this study, the term ‘wake’ without a qualifier refers to the ‘hydrodynamic wake’.

To visualise the area of influence of the monopile(s) on sediment dynamics and morphological processes, the first-order moment is used as a proxy for the hydrodynamic wake (i.e., the velocity deficit). This connection follows from the formulation of the sediment transport predictor used in the model (Soulsby, 1997), which is based on depth-averaged velocity. Since flow velocities are locally reduced downstream of the monopile, sediment transport capacity is directly lowered in those regions. The first-order moment, which reflects the magnitude of sediment transport over time, captures this reduction. Consequently, areas of reduced first-order moment correspond spatially to the wake zones, providing a meaningful and morphodynamically relevant representation of the wake influence.

To compute this, the sediment transport rate (a vector) is extracted at hourly intervals from simulations conducted both with and without wind turbine foundation(s). At each spatial point and time step, we calculate the vector difference between the two scenarios. The norm of this difference is then assigned a sign: a positive value indicates an increase in transport magnitude due to the monopile, while a negative value indicates a decrease, regardless of the direction of transport. This sign convention is intended to reflect the intuitive velocity deficits observed in the wake of monopiles, where transport may be reduced during one tidal phase (e.g., flood), even if net transport over the full cycle is enhanced. The use of a 360-day averaging period ensures that the moment calculation captures longer-term morphodynamic trends. Higher-order moments (variance, skewness, and kurtosis) were also calculated, but are not discussed here.

2.3.4 Assessment of annual dune migration

The impact of monopile(s) on seabed evolution, particularly on the propagation of marine dunes, is assessed by

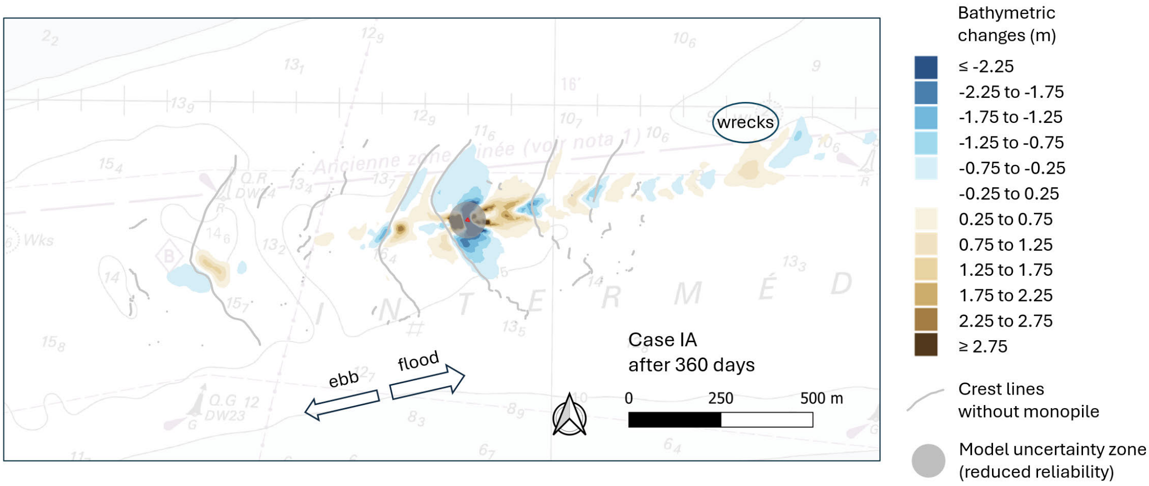

Figure 4 Bathymetric changes one year after the implementation of Case IA, calculated by subtracting the baseline seabed levels (without the monopile) from the levels with the monopile, both predicted after one year. The monopile location is shown as a filled triangle to scale. Shades of blue indicate lower seabed levels relative to the natural state, and shades of brown indicate higher levels. The greyed-out zone indicates an area of potential model uncertainty. Source of the background data: Shom nautical chart 7057.

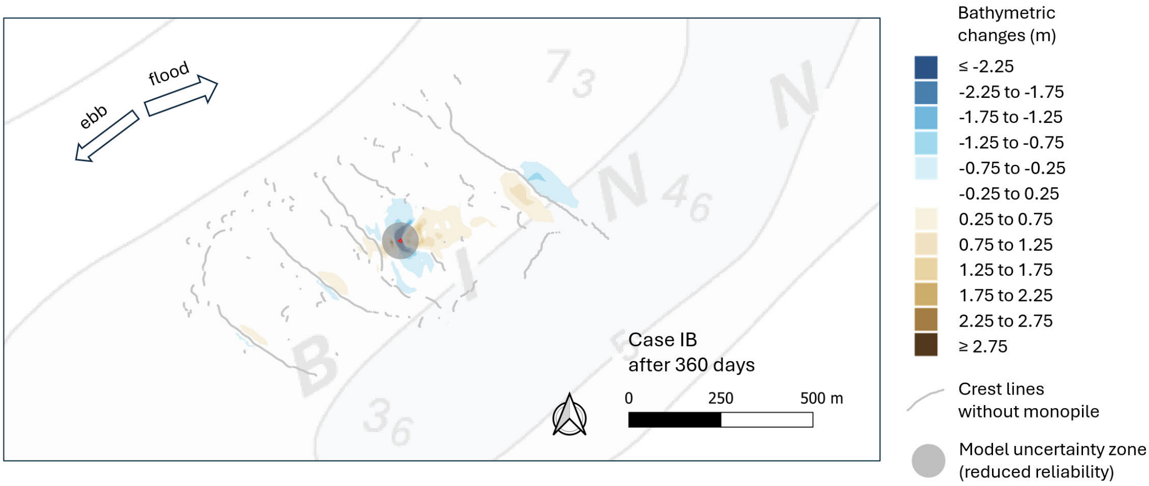

Figure 5 Bathymetric changes one year after the implementation of Case IB, calculated by subtracting the baseline seabed levels (without the monopile) from the levels with the monopile, both predicted after one year. The monopile location is shown as a filled triangle to scale. Shades of blue indicate lower seabed levels relative to the natural state, and shades of brown indicate higher levels. The greyed-out zone indicates an area of potential model uncertainty. Source of the background data: Shom nautical chart 7214.

comparing the (predicted) baseline DTM for the natural state with the (predicted) DTM including monopile(s). This analysis focuses on the first year of simulation. The resulting difference maps (e.g., Figures 4 and 5) highlight areas of seabed lowering and rising resulting from changes in bedform migration patterns. In these representations, white areas indicate regions where the presence of the monopile(s) shows no statistically significant deviation from natural erosion/accretion patterns.

To complement this analysis, the temporal evolution of specific transverse profiles is plotted through the monopile(s) for the entire simulation period (e.g., Figure 6). This representation allows for a synthetic visualisation of dune propagation as a function of time. A comparison of the predicted time evolution without and with monopiles gives insight into their effect.

In parallel, the dune crest lines are extracted to assess more precisely the impact on dune planform (for example, distortion and direction changes). For this, a spline is fitted to the seabed levels predicted by the model to add the resolution lacking from the model mesh (from 10 m to 1 m resolution). The resulting DTM is smoothed (SAGA 7.8.2 square 'simple filter') and is then used to extract local maximum values of seabed levels along transects spaced 0.5 m, applying a threshold to exclude secondary bedforms. This analysis is restricted to a few subset areas and times due to its high demands on computer time and disk space.

3 Results

3.1 Exploratory scenarios: Cases IA and IB

The predicted changes to the seabed one year after installing a single monopile within the dune field are depicted in Figure 4 (Case IA) and Figure 5 (Case IB). These changes are calculated as the difference in seabed levels with the monopile compared to the baseline scenario without the monopile. Each colour step represents a 0.5 cm variation, with lighter tones denoting smaller changes. Shades of blue indicate lower seabed levels than baseline and shades of brown indicate higher levels than baseline. The colour scale is designed to emphasise changes in the propagation of marine dunes, though local variations may exceed these limits (e.g., in the immediate vicinity of the foundation).

Wind turbine monopiles, like bridge piers, locally alter hydrodynamics, creating a complex 3D flow structure (e.g., Melville, 1988; Sumer and Fredsøe, 2002; Whitehouse, 1998). The increased turbulence can lead to the formation of a scour hole around the structure. It is important to note that these physical processes require much finer (horizontal and vertical) resolution than what is used here to model the large-scale propagation of marine dunes. Therefore, it cannot be expected that the local wake and other near-field processes are adequately represented in our model. To explicitly account for this limitation, we introduce a model uncertainty zone with a 50 m radius, five times the dominant mesh size of 10 m. This zone, indicated by a greyed-out area in all relevant figures, identifies the region where local seabed changes should be interpreted with caution.

As expected, the most significant morphological changes occur along the tidal axis and immediately around the monopile. Their spatial extent stabilises after an initial period of 90 to 180 days (not shown), but their magnitude increases with time. After one year, bed level variations greater than 0.25 m extend to 830 m west of the monopile and 900 m east of the monopile for Case IA (Figure 4). The largest predicted bed level variations (on the tidal axis, outside the greyed-out zone) are -1.6/+2.8 m west of the monopile and -1.4/+2.5 m east of the monopile. These variations, where bed changes approach full dune height, combined with the characteristic erosion-accretion patterns around the baseline crest locations (marked with grey lines), indicate significant dune migration.

There is a gradual accumulation of sediment in the streamwise direction in front of the monopile, particularly on the west side (+5.0 m in height after one year). This accumulation is consistent with the natural direction of sediment transport from west to east in Figure 4, due to the dominance of the flood currents. However, it appears to be exaggerated and is likely an artefact of the mesh resolution near the foundation, which limits the model ability to fully resolve local sediment processes. Over time, this leads to wave-like sediment deposition patterns close to the monopile, as shown in Figure 6b. In nature, these accumulated sediments might be expected to be drawn towards the scour hole and passed around the structure (Hong et al., 2017). To avoid misinterpretation from these numerical artefacts, we restrict our analysis to the first year of simulation.

One year after the installation of the monopile, the seabed changes are less pronounced for Case IB than for Case IA when compared to the baseline simulation without the monopile. Consistent with the lower dynamics observed in this area, the spatial extent of the seabed changes is also reduced compared to Case IA (approximately 500 m in each direction). The largest predicted changes in bed level (on the tidal axis, outside the greyed-out zone) are -0.3/+1.2 m southwest of the monopile and -0.6/+1.4 m northeast of the monopile (Figure 5).

The temporal evolution of the seabed, extracted along the tidal axis through the monopile, is illustrated in Figure 6 for Case IA (and in Figure S3 of Supplementary Materials for Case IB), where the dune crests naturally appear as lighter-coloured features. These figures corroborate our earlier observations that the navigation channel area is very dynamic (migration speed of 40–59 m/yr in the natural state), while the slopes of the Binnen Ratel sandbank are relatively less active (comparatively slower migration speed of 20–40 m/yr). The propagation is directed eastward, which is explained by stronger flood than ebb currents in these regions. The flow perturbation and initial bedform response begin immediately after the monopile is introduced in the model, but the distortion of the dune planform evolves steadily over time, consistent with the long-term linear progression shown in Figure 6.

Figure 6c, showing tracked crest positions from in situ measurements (crosses), the baseline (brown), and the monopile scenario (orange), clearly indicates that the seabed changes in Figure 4 correspond to the convergence of the dunes towards the monopile. The propagation is accelerated in areas where the general sediment transport was already directed towards the structure in the natural state (namely west of the monopile). Conversely, a reduction (Case IB, Figure S3) or even a reversal (Case IA) of the propagation is predicted in areas where the general direction of sediment transport was away from the structure (east of the monopile).

The displacement of the crests of the large marine dunes (Table S1, Supplementary Materials) quantifies this convergence after one year. The analysis uses a 2000-metre transect (as in Figures 6 and S3), so the table includes more dunes than shown in the seabed profiles of Figure 2. Displacement values are complemented by the acceleration rate, defined as the percentage change in dune migration speed (with vs. without the monopile) relative to the baseline speed. Negative values indicate deceleration (slower migration than the baseline), with values below -100% corresponding to a reversal of the migration direction. Table S1 reports that for Case IA, dunes west of the monopile accelerate by 73% on average, whereas those to the east decelerate severely (-164%), indicating a complete reversal of migration. In comparison, the effect is less pronounced for Case IB, with acceleration rates of 17% to the west and -73% (deceleration without reversal) to the east of the monopile.

3.2 OWF scenario: Case II

The changes to the seabed resulting from the implementation of the OWF offshore Dunkirk are illustrated in Figure 7 for Case II. The same colour scale as that used for Cases IA and IB is used to facilitate comparisons. In this representation, shades of blue indicate a decrease in seabed levels from the baseline levels without monopiles, and shades of brown indicate an increase in seabed levels at the end of one year.

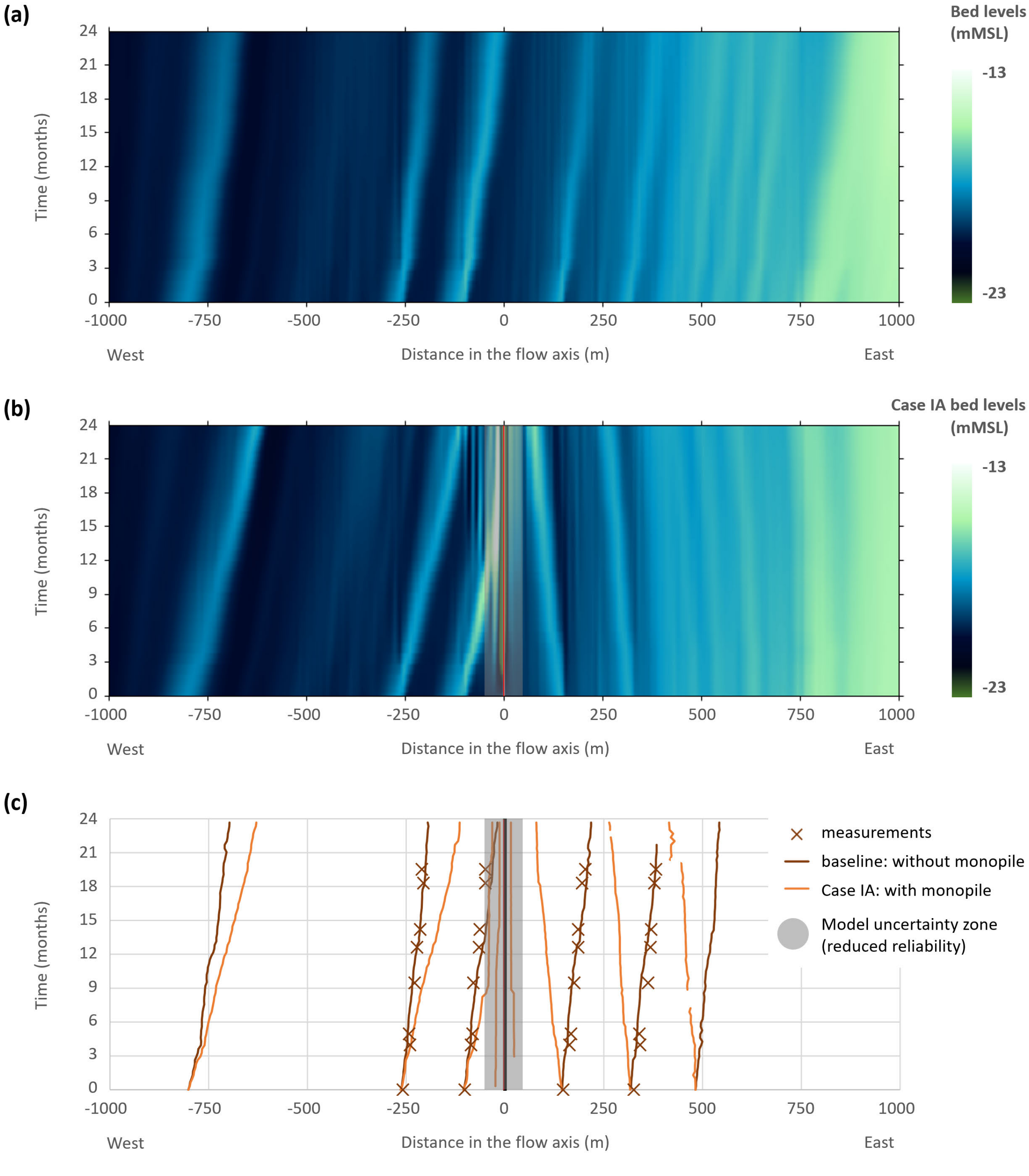

Figure 6 Temporal evolution of bed levels extracted along the tidal axis through the monopile (**a**) from the baseline simulation and (**b**) from the Case IA simulation, where the monopile is marked by the red line and the greyed-out zone indicates an area of potential model uncertainty. (**c**) Tracked dune crest positions, with crosses marking measured data from the bathymetric surveys conducted between November 2019 and July 2021 (FEM, 2021b).

Numerical instabilities are apparent on the steep slope of the Dyck Oriental sandbank (centre of Figure 7a), an area of high natural dynamics and steep gradients. These artefacts appear in both simulations with and without monopiles, confirming they are not induced by the foundations. They manifest early in the simulation, with bed-level oscillations typically ranging between $\pm$2–3 m after one year (approximately 10–15% of the local sandbank height). Although the magnitude of these oscillations increases with time, the instabilities remain localised and do not propagate to other areas of the computational domain. Outside this region, the most notable changes in seabed levels occur in the western part of the OWF, particularly between sandbanks (e.g., in Zone 1, Figure 7b) and on the Dyck Oriental sandbank (e.g., in Zone 2, Figure 7c).

In Zone 1, the wind turbines are placed in the gully between the Binnen Ratel and the Dyck Oriental sandbanks. The currents are channelised and very much bidirectional. Large marine dunes migrate in a south-

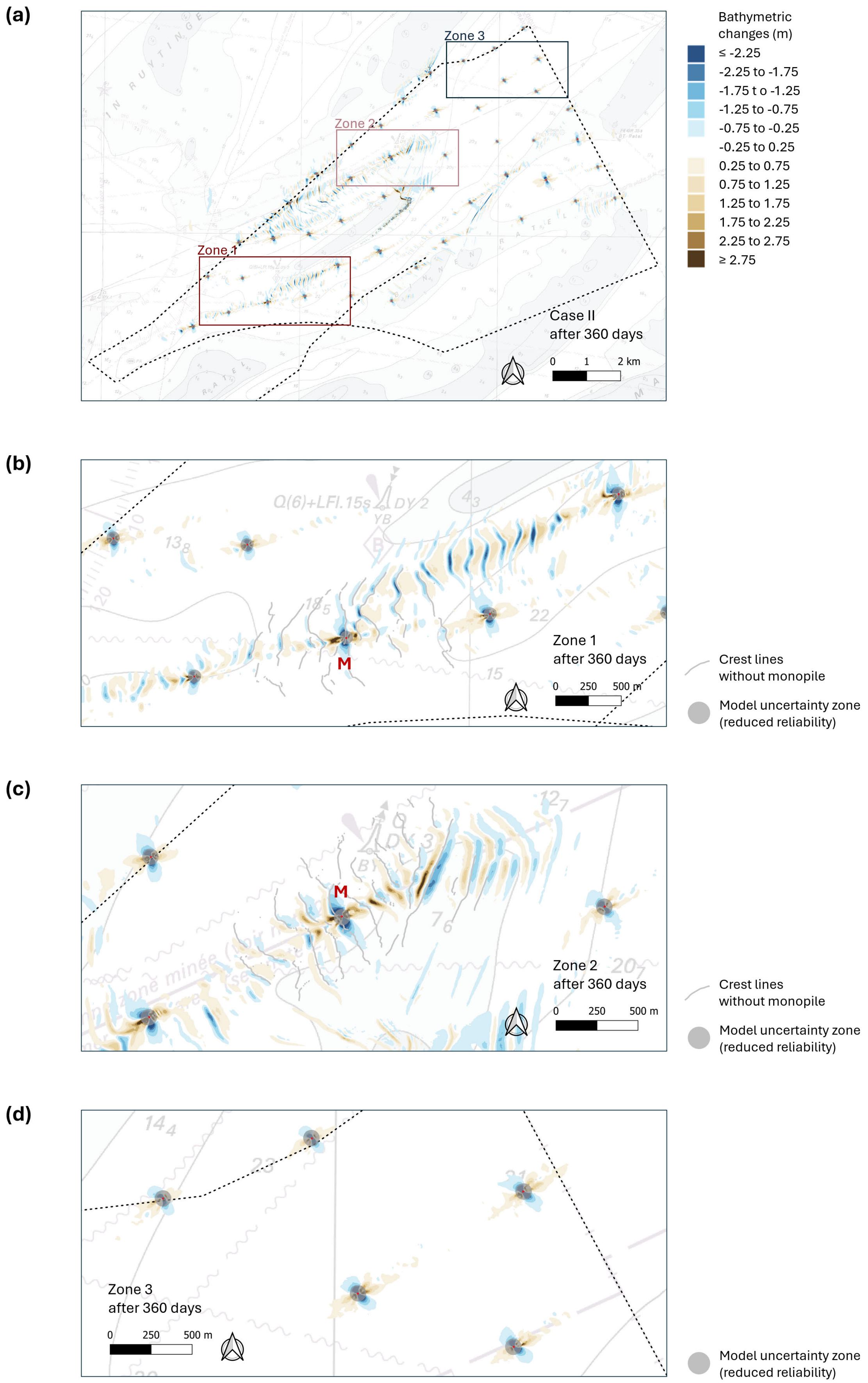

Figure 7 (**a**) Bathymetric changes one year after the implementation of Case II, calculated by subtracting the baseline seabed levels (without monopiles) from the levels with 46 monopiles, both predicted after one year. The 3 morphological behaviour zones defined in Figure 3b are identified by rectangles. Close-up views are presented for Zone 1 (**b**), Zone 2 (**c**) and Zone 3 (**d**), where each monopile is located at the centre of its greyed-out zone. Source of the background data: Shom nautical chart 7214.

westerly direction, contrary to the prevailing trend (Figure 3b). The area is dynamic, and the monopiles exert a significant influence on the surrounding environment (over more than 1 km), with the morphodynamic wake extending to adjacent wind turbines (Figure 7b). The rhythmic succession, in space, of seabed lowering and rising is testament to the impact on the marine dunes. The largest predicted variations in bed level (on the tidal axis of the monopiles, outside the greyed-out zone) are -1.8/+3.6 m west of the monopiles and -0.9/+3.3 m east of the monopiles. Variations of this magnitude indicate a significant difference in the position of the dunes without and with the monopiles, given that dunes in Zone 1 reach heights of 3 to 4 metres.

In Zone 2, the wind turbines are placed on the slopes of the Dyck Oriental sandbank. There, the prevailing currents align with the coastline but exhibit a wide range of directions corresponding to the turning of the tide. The morphodynamics of the area are complex, characterised by sediment transport directions that change by more than 90° within a short distance around buoy DY3 (Figure 3b), and dune morphology that transitions from 3D and northwest to southeast orientation to 2D and north-south orientation down the sandbank slope towards the gully. The bed changes shown in Figure 7c reflect these patterns. In this active area, the impact of the monopiles is again far reaching (more than 1 km). The largest variations are -1.5/+2.4 m either side of the monopile.

In Zone 3, in the northern corner of the OWF, the wind turbines are placed in a relatively flat and featureless area. The structures produce localised erosion on the sides of the monopiles due to vortex shedding and deposition along the flow axis (Figure 7d). These patterns typically develop in flat-bed tidal settings, as observed experimentally by Whitehouse and Stroescu (2023) and Wang et al. (2024). During one phase of the tidal cycle, the sediment that has been mobilised at the front of the monopile by the downflow and added turbulence is transported and deposited to the rear. With the reversal of the current in the subsequent tidal phase, the pattern is mirrored, with sediment from the new front side transported to the new rear side, resulting in sediment accretion on either side of the monopile. These depositional areas (indicated by brown shades in Figure 7d) grow steadily over time, reaching distances of 150–325 m after one year.

Zone 3 is excluded from further analysis due to the absence of large bedforms, which are the focus of this study. Instead, we concentrate on Zones 1 and 2. The temporal evolution of the seabed along transects passing through the monopile marked ‘M’ in Figure 7 is shown in Figures S4 and S5 of the Supplementary Materials, and the predicted displacement of marine dune crests is quantified in Table S2. The presence of monopiles alters the natural propagation of the dunes, which typically follows a west-southwest direction (Zone 1), causing them to converge on the structures. In Zone 2, this effect is superimposed on naturally variable migration directions. The influence of the monopile diminishes with distance: in Zone 1, for example, dune migration is redirected towards the structure only for the first 2 dunes west of the monopile (< 210 m), with acceleration rates as low as -171%. Further away, migration slows but does not reverse, with deceleration ranging from -55% to -89%. As a reminder, negative values indicate deceleration, and values below -100% a reversal of dune migration. In comparison, in Zone 2, the structure is predicted to have no impact on the furthest dune in the profile, west of the monopile (distance of ca. 800 m).

4 Discussion

4.1 Influence of OWF monopiles on annual dune migration

The impact of monopiles on hydrodynamics has been the subject of extensive investigation. The existence of distinct wake patterns in the lee of monopiles that disturb currents (Li et al., 2014; Miles et al., 2017; Rivier et al., 2016) and stratification (Cazenave et al., 2016; Schultze et al., 2020) has been demonstrated by field data, experimental data and numerical simulations. The streamwise extent of these patterns is dependent on the strength of the current and the size of the obstructing structure. While some studies have indicated a return to background levels by 10 pile diameters (Miles et al., 2017), satellite radar (SAR) imagery has revealed kilometre-scale surface current wakes downstream of offshore wind turbines (Li et al., 2014).

Questions remain about the impact of monopiles on sediment transport processes, in particular in live-bed regimes (characterised by sufficient flow velocities to continuously mobilise the seabed sediment). In the previous section, we demonstrated that the presence of monopiles creates a morphodynamic wake along the tidal axis, causing the dune planform to distort and converge towards the structure. We will now explore the underlying mechanisms responsible for this effect.

Consider a monopile placed in an environment with a steady current fast enough to support dune movement. In the downstream wake of the structure, the flow velocity is lower compared to the surrounding areas (e.g., Li et al., 2014; Rivier et al., 2016). Since sediment transport depends on flow velocity, the dune moves forward more slowly in the hydrodynamic wake than in other regions.

Now, consider that the current changes direction with the following phase of the tide. The downstream becomes the new upstream and vice versa; the sedimentary process is mirrored. If the currents are stronger during one phase of the tidal cycle than during the other, the dune naturally travels in the direction of the net flow (Fredsøe and Deigaard, 1992; van Gerwen et al., 2018). The downstream wake created in turn by each tidal phase causes the section of the dune on the flow axis to converge towards the structure, while the rest of the dune moves at its natural speed in other areas.

This mechanism, which we introduce as the ‘wake effect’, is illustrated schematically in Figure 8. The predominance of the flood (directed to the right in this sketch) is materialised by a brown net sediment transport vector outside the monopile wake. As a result, the dunes travel to the right, and the position of the dune

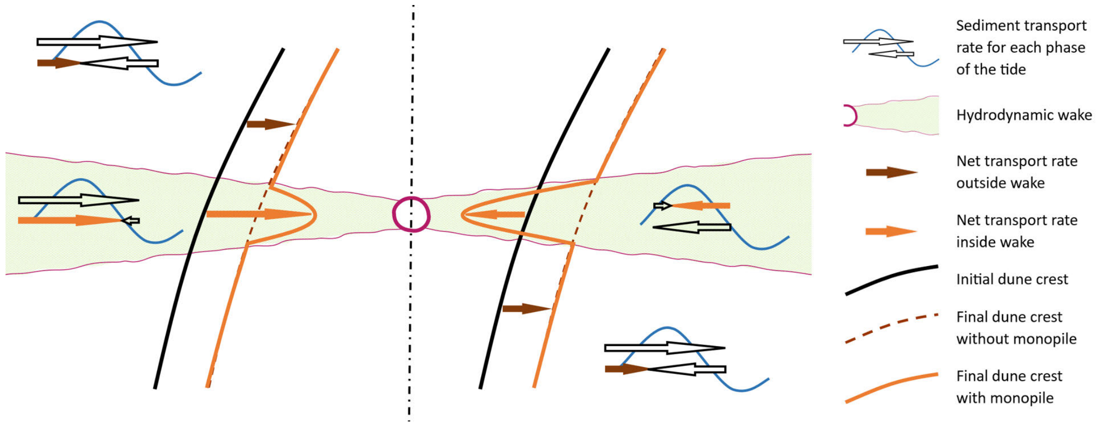

Figure 8 Schematic representation of the influence of a monopile on net sediment transport rates (filled arrows) and marine dune migration (lines). Brown shows the natural state without a monopile, and orange the modified state due to the inclusion of a monopile (area of influence indicated by shading). The natural direction of dune migration is from left to right.

crest after some time is indicated by a dashed brown line. In the hydrodynamic wake, however, shown as a shaded area, the net sediment transport vector is modified (orange). It becomes stronger to the left of the obstacle due to the reduction of the opposing ebb sediment transport vector, and weaker to the right of the obstacle due to the reduction of the dominant flood sediment transport vector. These changes cause the dune migration to accelerate as the dunes approach the monopile and to slow or even reverse as they migrate away. The resulting position of the dune crest in the monopile wake is indicated by a solid orange line.

The wider the tidal ellipse at the site, the less focused the impact of the monopile. The further the monopile from the dune, the less pronounced its impact. Similarly, a streamlined structure is expected to reduce the hydrodynamic wake (Aly and Dougherty, 2021), thereby minimising the 'wake effect' on dune propagation.

This 'wake effect' differs from the mechanism described by Hong et al. (2017) for linear dunes approaching a monopile with an already formed scour hole under steady currents. Based on experimental observations, such as those by Chiew (1984), the authors indicate that the dune section upstream of the monopile is drawn into the scour hole. The increased turbulence at the base of the structure then picks up and transports the sediment, resulting in a higher transport rate compared to the areas around the monopile. This leads to a stretched, elongated planform in the streamwise direction.

It is conceivable that both mechanisms coexist in reality. However, the seabed changes documented in Section 3 cannot be attributed to scour processes alone. This conclusion (that local scour is an incomplete explanation) is consistent with the observations made by Couldrey et al. (2020), who found that large-scale hydrodynamic variability contributed to the stretching of an isolated crescent-shaped dune off the east coast of the UK. While their study did not report far-field attraction of dunes towards the foundation, it supports the notion that mechanisms beyond local scour may influence bedform evolution.

Not shown in Figure 8 for clarity, the presence of the monopile not only creates a hydrodynamic wake but also causes the flow to deviate and increase around the sides of the structure (e.g., Rivier et al., 2016). This localised flow acceleration may enhance sediment transport and lead to a corresponding increase in dune migration rates in these areas; however, such effects are spatially limited and not the focus of the present analysis.

The 'wake effect' on annual dune propagation is depicted in Figure 9 for Case IA and for Case II in Zone 1. In Case IA, a monopile was placed in the navigation channel to Dunkirk. During the flood phase, currents trend east-northeast, while during the ebb phase, they trend west-southwest. The natural sediment transport pathway and the progression of the dune, driven by the stronger flood, are directed east-northeast (Durand et al., 2025; Le Bot et al., 2023). The presence of the monopile modifies the velocity and consequently the distribution of sediment transport along the tidal axis. Green shades indicate a decrease in the first-order moment of sediment transport (see Section 2.3.3 for calculation), attributed to a reduction during one of the tidal phases. This distorts the dune planform by drawing the dunes towards the monopile (Figure 9), as previously explained. At the same time, while the heights remain mostly unchanged, the dune cross-sectional profile is modified with steep slopes facing the monopile on either side (not shown). Green shades are associated with convergence. In contrast, pink lobes indicate an increase due to flow acceleration around the sides, resulting in an accelerated migration of the dune. Pink shades are associated with divergence.

In Case IB (not shown), a monopile was placed on the slope of the Binnen Ratel sandbank. The natural sediment transport pathway and dune progression are also directed east-northeast, but the seabed there is less mobile (Durand et al., 2025) – likely due to weaker currents and a wider tidal ellipse. Consequently, the 'wake effect', while still apparent, is less pronounced.

Interpreting dune behaviour in Case II is considerably more difficult due to the number of monopiles in the array and the competing 'wake effect' each monopile exerts on different sections of the dunes. This complexity is illustrated in Figure 9b (note the different colour scale) for monopiles located in the gully between the

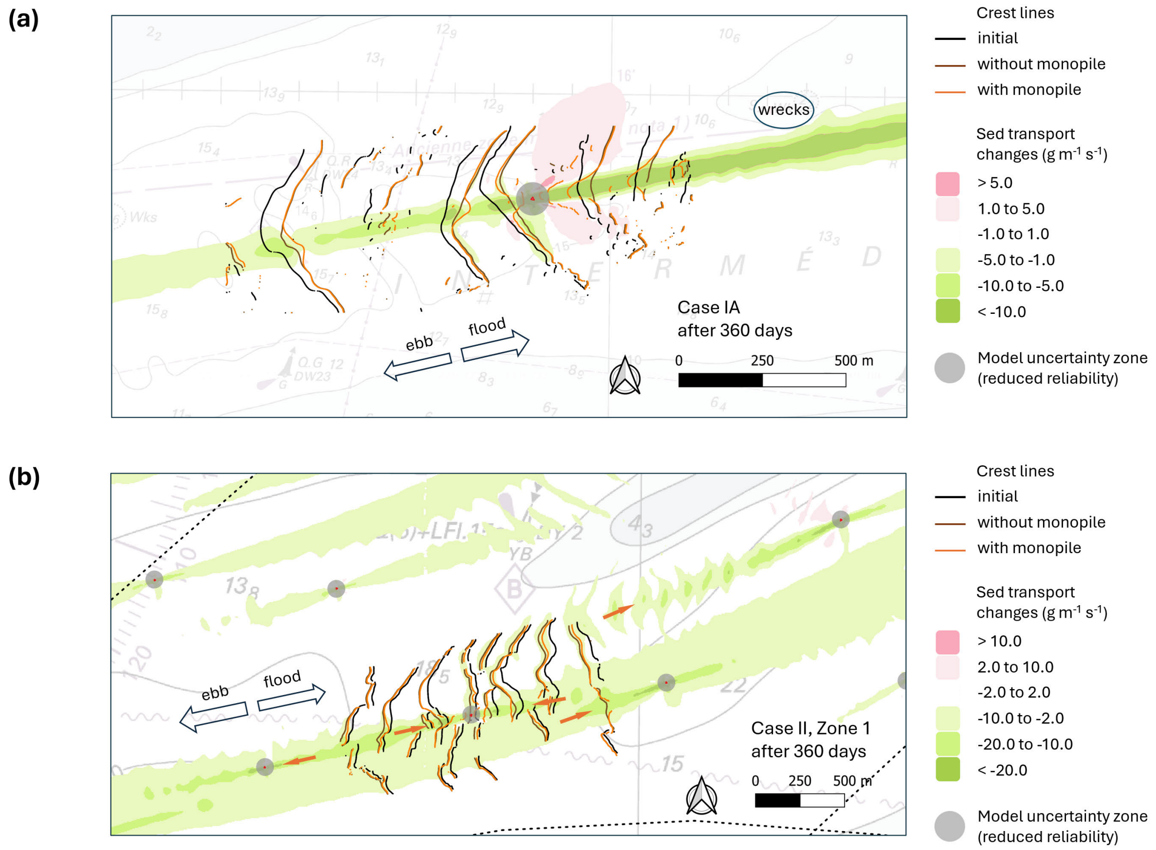

Figure 9 Crest line distortion on the tidal axis of the monopiles after one year: (**a**) for Case IA and (**b**) for Case II, Zone 1. The monopile locations are shown as filled triangles to scale and the greyed-out zones indicate areas of potential model uncertainty. Source of the background data: Shom nautical charts 7057 and 7214.

Binnen Ratel and Dyck Oriental sandbanks, in the area we refer to as Zone 1. For clarity, not all dune crests are shown in this figure. Orange arrows identify sections that are drawn east-northeast (because the dominant flow is reduced in the monopile wake) and others that are drawn west-southwest (because the opposing flow is reduced) in comparison to the natural progression of the dunes.

It is important to recognise that the first-order moment of sediment transport alone may not fully capture the impact of hard, immobile structures like monopiles on dune migration. Changes in the kinetics of dune propagation are observed beyond the coloured areas of influence. For instance, in Case IA, the second and third crescent-shaped dunes north of the wakes (Figure 9a) migrate at a slightly slower speed when the monopile is in place compared to the baseline. This would be consistent with increased sediment transport around the monopile during ebb flows (we might expect two lobes either side of the tidal axis similar to the flood), but this is not reflected in the first-order moment, even with a finer colour scale.

4.2 Impact in relation to the natural variability of sedimentary processes

It is useful to consider the impact of monopiles in the context of natural variability in sedimentary processes. Dune migration, in particular, is influenced by meteorological conditions (Campmans et al., 2018; Harris, 1991; Le Bot and Trentesaux, 2004). Offshore Dunkirk, Durand et al. (2025) have suggested a 36% increase in dune migration rate in winter compared to the entire year. This seasonal variability is reflected in the temporal evolution plots presented in Figure 6 and the Supplementary Materials, which show periods of accelerated and decelerated migration, as well as periods of reversed migration. For example, dune positions remained stable between month 4 (17-Mar-2020) and month 7 (17-Jun-2020), a period marked by an unusual spring. While winds from the southwest prevail annually, the proportion of northeasterly winds typically increases in spring due to cold fronts from Scandinavia, reaching approximately 20%. In spring 2020, however, this proportion rose to nearly 50%, explaining the stabilisation observed between mid-March and mid-June.

Durand et al. (2025) calculated the natural migration speed of the crescent-shaped dune nearest to the Case IA monopile, for each time step in a one-year simulation of the baseline. We conducted a similar analysis for the period from December 2019 to November 2020, in the OWF area for dune (sections) just west of the Case II monopiles labelled 'M' in Zones 1 and 2. The monthly variability in migration speed can be evaluated from these hourly data. The results are shown in Figure 10 as brown lines for the natural state (without turbine foundations). Since we use calendar months, the careful reader will note a slight discrepancy with the data presented in Figures S4 and S5, where the zero time is the start of the simulation, i.e., 17-Nov-2019.

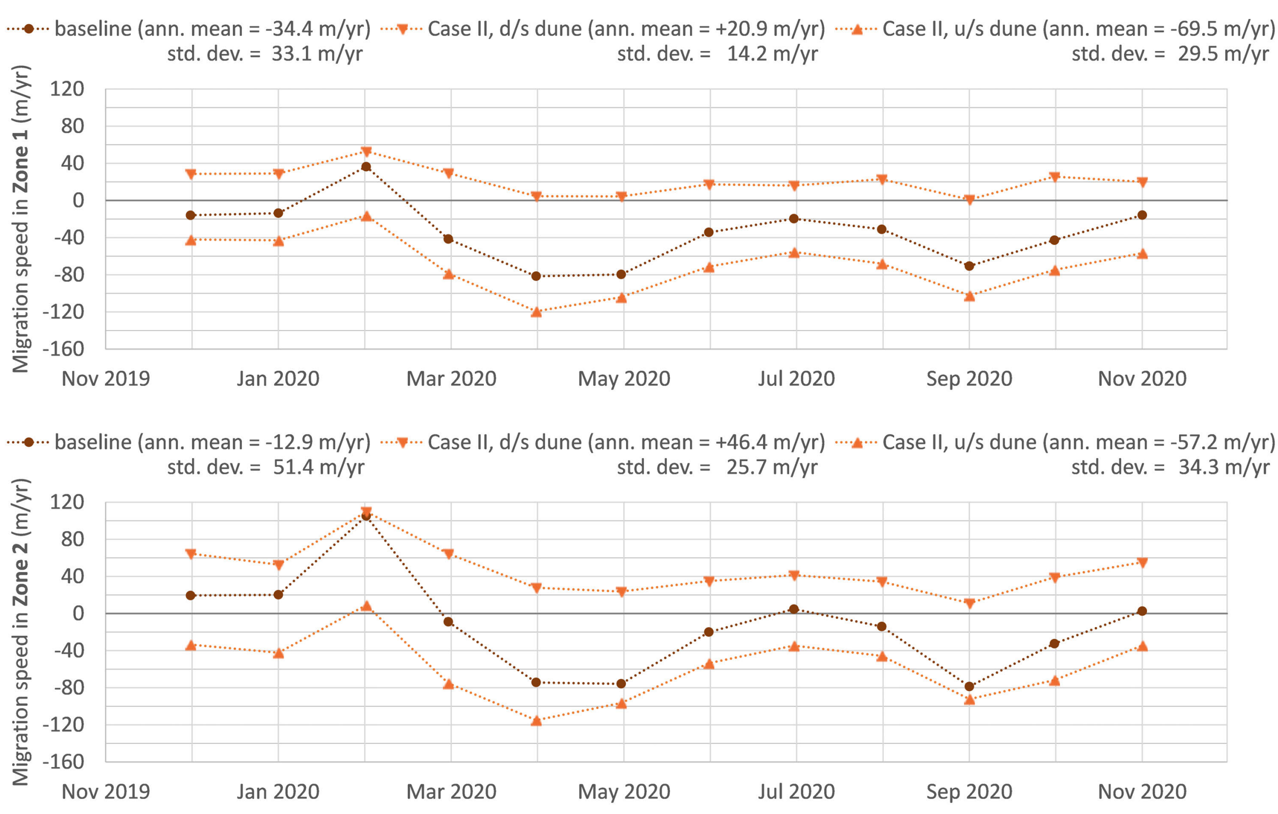

Figure 10 Seasonal variability in the dune migration speed in Zones 1 and 2 of the OWF area (Figure 3), comparing the natural state (brown) and the modified state with an array of monopiles (orange). The upward triangles (▲) track a dune located just upstream (u/s) of the monopile; the downward triangles (▼) track a different dune located just downstream (d/s).

These results indicate significant variability in the migration speed of the dunes. Such variability is not unusual; for example, Lanckneus and de Moor (1991) documented a case on the northern Kwintebank (Belgian continental shelf) where dunes migrated 28 m in one direction over 4 months, followed by 29 m in the opposite direction over the next 5 months (resulting in a net annual migration close to zero). Some variability is also observed in the direction of migration, particularly in Zone 2, identified earlier as an area where the sediment transport vectors were turning. The dune selected for the analysis there travels towards the east-northeast during winter (positive speed according to our convention) but towards the west-southwest for the remainder of the year.

For the Case II simulation with monopiles, we calculated the migration speed for both the same downstream dune section (▼) tracked in the natural state, and for a new, adjacent dune located immediately upstream/east of the monopile (▲). Averaged over a year, dune migration accelerates upstream of the monopile, with increases of 102% and 343% in Zones 1 and 2, respectively. Conversely, migration direction reverses downstream of the monopile, evidenced by annual rates < -100%, with values reaching -161% in Zone 1 and -460% in Zone 2. These results, shown in Figure 10 as orange lines, demonstrate a significant impact of monopiles, with modified migration speeds clearly falling outside the range of natural (seasonal) variability in proximity to the structures. The magnitude of this impact, up to a factor of 4 close to the monopile, extends several hundred metres (see Table S2), but decreases with increasing distance from the structure.

4.3 Implications of turbine placement (cumulative effect)

Strategic placement of wind turbines within an array is crucial for several reasons. Firstly, it ensures that the turbines are not positioned in the atmospheric wake of the upstream units (Frandsen et al., 2006; Stevens and Meneveau, 2017), thus maximising the efficiency of the wind resource. Typically, turbines are spaced 8–10 times the rotor diameter in the prevailing wind direction and 3–5 times in the perpendicular direction (Bhattacharya, 2019). Furthermore, careful placement aims to reduce construction and installation costs, particularly by optimising the electrical system and minimising the length of intra-array and export cables (Hou et al., 2019). Separately, micro-siting of wind turbines plays an important role in minimising the environmental impact on marine life and seabed ecosystems. By carefully selecting turbine locations, the overall region of hydro- and/or morphodynamic influence of the OWF can be reduced, and sensitive areas avoided.

Elongated monopile wakes are predicted in Case IA (Figure 9a, single monopile), with lengths consistent with recent observations of kilometre-scale sediment plumes by Li et al. (2014) in the East China Sea, and by Vanhellemont and Ruddick (2014) and Forster (2018) at offshore wind farms in the southern North Sea (UK). To investigate cumulative effects of multiple monopiles,

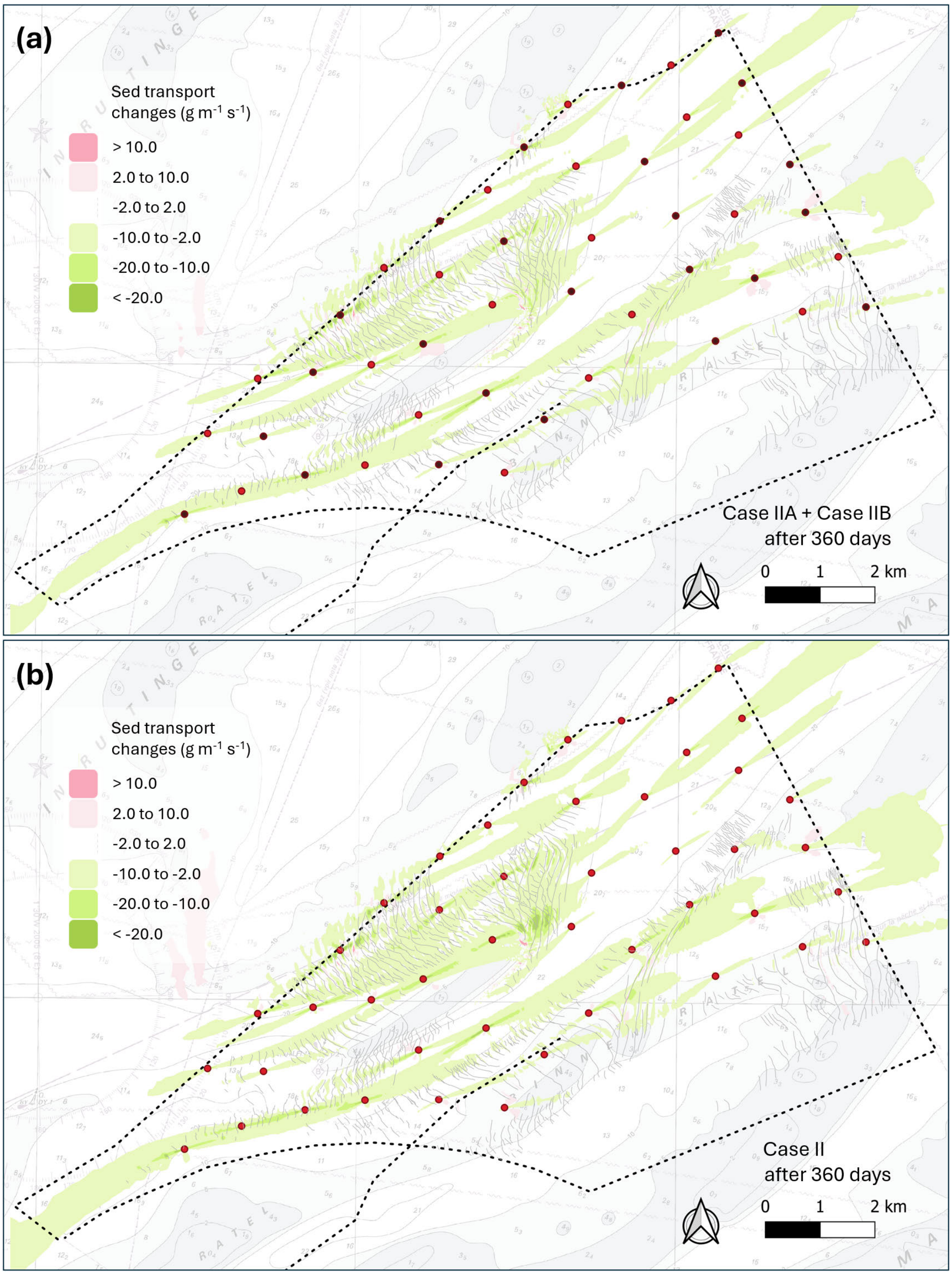

Figure 11 Area of influence of monopiles considered (**a**) individually in two half-array configurations: Case IIA (monopile locations shown as black circles) and Case IIB (red circles), or (**b**) collectively in a full offshore wind farm array (Case II), illustrating the cumulative effect of the turbine placement. The first-order moment of sediment transport rate is used as an indicator of the 'wake effect.'

we modelled a full array of 46 turbines in Case II, with a relatively dense spacing of approximately 1000 m. In this configuration, wake interference is anticipated as the wakes associated with the first-order moment of sediment transport are predicted to exceed the spacing between neighbouring wind turbines, potentially affecting upstream units.

To isolate and better understand these interactions, we introduced two additional scenarios: Cases IIA and IIB, each representing half-array configurations. These subsets were designed to avoid overlapping effects a priori, allowing clearer attribution of individual monopile impacts. The cumulative effect of these two half-array cases is shown in Figure 11a, and compared with the impact predicted for the entire array in Figure 11b. The difference between these configurations highlights the non-linear nature of wake interference and sediment redistribution across the array.

Wake effects are associated with areas where mobile bedforms, such as marine dunes, are present. These regions are more susceptible to morphodynamic changes than areas with a stable or featureless seabed. The wider stripes of change observed in Figure 11b under the full-array scenario are a result of wake interference, where overlapping wakes from closely spaced turbines interact laterally. This is particularly evident in the gully between the Binnen Ratel and Dyck Oriental sandbanks (Figure 7b), where the row-wise arrangement of the wind turbines amplifies sediment transport changes. Another area where significant changes are predicted is the region southwest of Zone 2 (Figure 7a). The darker shades of green in this region indicate increased morphodynamic change when all structures are considered collectively rather than individually. This suggests that the placement of wind turbines must be carefully considered to minimise impacts on sediment dynamics, dune propagation, and more generally, on marine life and seabed ecosystems (Isaksson et al., 2023).

4.4 Remarks about the design of the study

This study employed a 3D hydrodynamic model coupled with a sediment transport and bed evolution model to investigate interactions between large marine dunes and offshore wind farm fixed foundations (monopiles). While the approach successfully reproduced natural dune propagation patterns (Durand et al., 2025), several methodological aspects merit discussion, particularly given the absence of field data for direct validation of dune–monopile interactions.

A key aspect of the model is the use of the Soulsby-van Rijn predictor (Soulsby, 1997), which relies on depth-averaged velocity rather than bed shear-stress. The formulation is grounded in energy-based transport principles (Bagnold, 1966; van Rijn, 1984), where bedload transport rates scale with flow kinetic energy. Under current-dominated conditions (without waves), it simplifies to van Rijn's (1984) parameterisation, incorporating logarithmic boundary layer scaling. This depth-averaged approach inherently captures transport maxima over dune crests, enabling realistic migration without requiring explicit near-bed resolution. Its effectiveness has been demonstrated in the Dunkirk area to simulate the migration of marine dunes over a 13-month period (Durand et al., 2025). This is further supported by Lokin et al. (2023), who showed that a different depth-averaged predictor (Engelund and Hansen, 1967) was able to simulate river dune propagation, reinforcing the general capability of mean-flow-based predictors for bedform migration.

The influence of local seabed slope on bedload transport (both in magnitude and direction) was disabled to focus on advective migration processes. Although this simplification omits a known balancing mechanism in natural dune systems (Borsje et al., 2014), the only theoretically compatible slope correction introduced a second-order bed elevation derivative (acting as diffusion), which led to unrealistic dune decay in the natural state (Durand et al., 2023b).

Another pragmatic design choice was the vertical resolution of the model, limited to 5 layers for computational efficiency. While standard practice typically suggests $\geq$20 layers to resolve finer-scale circulation affecting, for example, dune growth, our focus on migration and the energy-based framework justified a more streamlined representation (Durand et al., 2023b). The model does not aim to fully resolve near-foundation processes or the full complexity of natural dune systems, as mesh resolution limits the representation of local sediment dynamics. Future work could incorporate stress-based predictors, slope-induced transport, and sensitivity analyses of vertical resolution to better capture recirculation mechanisms. Nonetheless, the current setup offers a computationally efficient framework aligned with the study objectives.

Validation remains a challenge in the absence of field data, as construction at Dunkirk has not yet begun. To our knowledge, no extensive, recurrent bathymetric surveys exist for offshore wind farms with comparable conditions (sandy seabed, $\sim$20 m water depths, currents up to 1.25 m/s) and monopile foundations. Post-construction surveys typically prioritise scour monitoring (Couldrey et al., 2020) or cable integrity rather than dune propagation. Given the lack of repeated site-specific data at Dunkirk, a sequential modelling strategy was implemented: initial simulations focused on single-monopile scenarios in well-characterised, data-rich environments where baseline morphodynamics could be validated; subsequent simulations incorporated the full turbine array of the Dunkirk OWF. While the differing locations reflect practical constraints, the design provides complementary insights into dune-foundation interactions.

The model was not applied to long-term (decadal) morphodynamic evolution. Results are shown after one year of simulation to highlight persistent large-scale effects, such as dune migration speed and bedform reorganisation. By design, the model reliability decreases near the monopiles due to unresolved fine-scale processes. Consequently, local predictions of scour depths and immediate wake effects should be interpreted as indicative, a limitation visualised by the greyed-out areas in the figures. The model is best suited for broader-scale process understanding, and the results lay the groundwork for future studies once field observations from operational wind farms become available.

5 Conclusions

A large-scale numerical model, using the process-based open**TELEMAC** system, combines 3D hydrodynamics with a depth-averaged sediment transport approach to investigate the impact of offshore wind foundations on annual dune migration. This model is applied to a large coastal area in the Southern Bight of the North Sea, where a 600 MW offshore wind project is planned. The area is subject to strong tidal flows and winds originating from the Atlantic Ocean and the North Sea. Marine dunes and sandbanks are present within the wind farm area, with dune migration rates of up to 30 m/year.

Our findings indicate that monopiles significantly affect their environment, causing sections of the dunes along the tidal axis to converge towards the monopile, while those outside of the wake continue moving at their natural speed. In a realistic scenario with 46 wind turbines, each monopile in the array exerts a competing impact on sections of the dune.

We have termed this convergence towards the monopile 'wake effect', which refers to the down-current velocity deficit and subsequent reduction in sediment transport during a tidal phase. This results in increased migration rates when dunes approach the monopile and decreased rates (or even reversal) when migrating away from it.

Although there is considerable natural variability in seasonal dune migration due to meteorological influences, the impact of the monopiles is predicted to exceed this variability. Dune propagation is either accelerated or reversed, with changes reaching up to a factor of 4 close to the foundation.

The cumulative impact of the monopiles on the first-order moment of sediment transport, which we use as an indicator of the 'wake effect', underscores the need for careful placement of the wind turbines in the array to avoid or, at the very least, mitigate the effects on the dune field.

These results contribute to our understanding of the interaction between fixed offshore wind foundations and marine dunes at an intermediate scale that fits between the broader wind farm level and the more localised monopile level. While not intended for long-term morphodynamic predictions, they help to bridge the gap between these two commonly considered approaches.

Acknowledgements

The authors thank the partners of the MODULLES project for providing site-specific data and giving permission to publish this work.

Land Recognition

The authors confirm that the lands where their institutions are located, as well as all sites related to this study, hold no known cultural or historical significance to any specific Indigenous group.

Data and Codes Availability

The openTELEMAC system used in this research can be downloaded from https://opentelemac.org/. Large-scale bathymetric data from the French Naval Hydrographic and Oceanographic Service are publicly available at https://diffusion.shom.fr/donnees/bathymerie/mnt-facade-atl-homonim.html and https://diffusion.shom.fr/donnees/bathymerie/mnt-topo/mnt-cotier-pas-de-calais.html. Older hydrodynamic and sedimentary data mentioned in this article have been released and are available from Shom (2017a,c). The recent metocean and bathymetric data collected specifically for this project are not currently available to the public or research community. Access can be requested from France Energies Marines (https://www.france-energies-marines.org/contact/).

Funding Statement

N.D. was supported by France Energies Marines, through the MODULLES project. MODULLES is co-funded by the French National Research Agency as part of the France 2030 Investment Plan, under reference number ANR-10-IEED-0006-34, and by France Energies Marines and its members. Computer time was provided under the EDF R&D POWERX project.

Conflict of Interest Disclosure

The authors declare that they have no known competing interests, financial or otherwise, that could have appeared to influence the work reported in this paper.

Permission to Reproduce Material from Copyrighted Sources

The authors declare that no material from copyrighted sources was reproduced in this manuscript.

Declaration on Artificial Intelligence Use

The authors declare that no artificial intelligence (AI) tools were used to generate any substantive content in this manuscript. However, large language models (LLMs) were occasionally used to assist with writing style, grammar, and language refinement.

References

Aly, A. M. and Dougherty, E. Bridge pier geometry effects on local scour potential: A comparative study. *Ocean Engineering*, 234:109326, 2021. doi: https://doi.org/10.1016/j.oceaneng.2021.109326.

Ashley, G. M. Classification of Large-Scale Subaqueous Bedforms: A New Look at an Old Problem - SEPM Bedforms and Bedding Structures. *Journal of Sedimentary Petrology*, 60(1):160–172, 1990. doi: https://doi.org/10.2110/jsr.60.160.

Bagnold, R. A. An approach to the sediment transport problem from general physics. *Geological Survey Professional Paper*, 422 (I), 1966. doi: https://doi.org/10.3133/pp422I.

Bartholdy, J., Bartholomä, A., and Flemming, B. W. Grain-size control of large compound flow-transverse bedforms in a tidal inlet of the Danish Wadden Sea. *Marine Geology*, 188(3):391–413, 2002. doi: https://doi.org/10.1016/S0025-3227(02)00419-X.

Bhattacharya, S. *Design of Foundations for Offshore Wind Turbines*. John Wiley & Sons, 2019. doi: https://doi.org/10.1002/9781119128137.

Borsje, B. W., Kranenburg, W. M., Roos, P. C., Matthieu, J., and Hulscher, S. J. M. H. The role of suspended load transport in the occurrence of tidal sand waves. *Journal of Geophysical Research: Earth surface*, 119(4):701–716, 2014. doi: https://doi.org/10.1002/2013JF002828.

Bouttier, F. Arome, avenir de la prévision régionale. *La Météorologie*, (58):12–20, 2007. doi: https://doi.org/10.4267/2042/18203.

Campmans, G. H. P., Roos, P. C., Schrijen, E. P. W. J., and Hulscher, S. J. M. H. Modeling wave and wind climate effects on tidal sand wave dynamics: A North Sea case study. *Estuarine, coastal and shelf science*, 213:137–147, 2018. doi: https://doi.org/10.1016/j.ecss.2018.08.015.

Cazenave, P. W., Torres, R., and Allen, J. I. Unstructured grid modelling of offshore wind farm impacts on seasonally stratified shelf seas. *Progress in Oceanography*, 145:25–41, 2016. doi: https://doi.org/10.1016/j.pocean.2016.04.004.

Chiew, Y. M. *Local scour at bridge piers*. Phd thesis, University of Auckland, 1984.

Clark, S., Schroeder, F., and Baschek, B. The influence of large offshore wind farms on the North Sea and Baltic Sea - a comprehensive literature review. Technical Report HZG Report 2014-6, Helmholtz-Zentrum Geesthacht, 2014.

Cooper, B. and Beiboer, F. Potential effects of offshore wind developments on coastal processes. Technical Report URN 02/1336, ABP Marine Environmental Research Ltd, 2002.

Couldrey, A. J., Benson, T., Knaapen, M. A. F., Marten, K., and Whitehouse, R. J. S. Morphological evolution of a barchan dune migrating past an offshore wind farm foundation. *Earth Surface Processes and Landforms*, 45:2884–2896, 2020. doi: https://doi.org/10.1002/esp.4937.

Durand, N., Tassi, P., Blanpain, O., and Lefebvre, A. Understanding marine dune dynamics in a shallow shelf sea using sediment mobility indices. In *Marine and River Dune Dynamics VII Book of Proceedings*, pages 109–116, 2023a. April 1-3, 2023. Rennes, France.

Durand, N., Tassi, P., Blanpain, O., and Lefebvre, A. GAIA can model large marine dunes: Results from a sensitivity study in the southern North Sea. In *XXIXth Telemac-Mascaret User conference*, pages 190–197, 2023b. October 12-13, 2023. Karlsruhe, Germany.

Durand, N., Tassi, P., Blanpain, O., and Lefebvre, A. Meteorological Conditions Influence the Migration of a Marine Dune Field in the Southern North Sea. *Journal of Geophysical Research: Earth Surface*, 130(1):e2024JF007731, 2025. doi: https://doi.org/10.1029/2024JF007731.

EMD. June 2021 multi-beam bathymetric survey conducted as part of pre-feasibility studies for the Dunkirk offshore wind farm area. Proprietary data not available to the public at this time, 2021.

EMD. 2021-2022 wind, pressure, level, current and wave measurements collected as part of pre-feasibility studies for the Dunkirk offshore wind farm area. Proprietary data not available to the public at this time, 2022.

Engelund, F. and Hansen, E. A monograph on sediment transport in alluvial streams. Technical Report Hydraulic Engineering Report, Technical University of Denmark, 1967.

European Environment Agency (EEA) coastline, version 3.0. https://www.eea.europa.eu/data-and-maps/data/eea-coastline-for-analysis-2/, Last accessed January 6, 2022.

FEM. 2019-2020 bed samples collected as part of pre-feasibility studies for the Dunkirk offshore wind farm area (DUNES project). Proprietary data not available to the public at this time, 2020.

FEM. 2021 level and current measurements collected as part of pre-feasibility studies for the Dunkirk offshore wind farm area (DUNES project). Proprietary data not available to the public at this time, 2021a.

FEM. 2019-2021 multi-beam bathymetric surveys conducted as part of pre-feasibility studies for the Dunkirk offshore wind farm area (DUNES project). Proprietary data not available to the public at this time, 2021b.

Flemish Hydrography - Maritime and Coastal Services. Depth model Belgian Continental Shelf and nautical data. https://www.vliz.be/en/datasets-belgian-coast-and-sea?module=dataset&dasid=5643, 2022.

Forster, R. M. The effect of monopile-induced turbulence on local suspended sediment patterns around UK wind farms: field survey report. Technical Report IECS-YBB313-2017, Institute of Estuarine & Coastal Studies (IECS), 2018.

Frandsen, S., Barthelmie, R., Pryor, S., Rathmann, O., Larsen, S., Højstrup, J., and Thøgersen, M. Analytical modelling of wind speed deficit in large offshore wind farms. *Wind Energy*, 9(1-2): 39–53, 2006. doi: https://doi.org/10.1002/we.189.

Fredsøe, J. and Deigaard, R. *Mechanics of Coastal Sediment Transport*. World Scientific, 1992. doi: https://doi.org/10.1142/1546.

Games, K. P. and Gordon, D. I. Study of sand wave migration over five years as observed in two windfarm development areas, and the implications for building on moving substrates in the North Sea. *Earth and Environmental Science Transactions of the Royal Society of Edinburgh*, 105(4):241–249, 2014. doi: https://doi.org/10.1017/S1755691015000110.

Harris, P. T. Reversal of subtidal dune asymmetries caused by seasonally reversing wind-driven currents in Torres Strait, northeastern Australia. *Continental Shelf Research*, 11(7):655–662, 1991. doi: https://doi.org/10.1016/0278-4343(91)90018-2.

Hervouet, J.-M. *Hydrodynamics of free surface flows : Modelling with the finite element method*. John Wiley & Sons, 2007. doi: https://doi.org/10.1002/9780470319628.

Hong, J.-H., Chiew, Y. M., Yeh, P.-H., and Chan, H.-C. Evolution of Local Pier-Scour Depth with Dune Migration in Subcritical Flow Conditions. *Journal of Hydraulic Engineering*, 143(4), 2017. doi: https://doi.org/10.1061/(ASCE)HY.1943-7900.0001261.

Hou, P., Zhu, J., Ma, K., Yang, G., Hu, W., and Chen, Z. A review of offshore wind farm layout optimization and electrical system design methods. *Journal of Modern Power Systems and Clean Energy*, 7(5):975–986, 2019. doi: https://doi.org/10.1007/s40565-019-0550-5.

Isaksson, N., Scott, B. E., Hunt, G. L., Benninghaus, E., Declerck, M., Gormley, K., Harris, C., Sjöstrand, S., Trifonova, N. I., Waggitt, J. J., Wihsgott, J. U., Williams, C., Zampollo, A., and Williamson, B. J. A paradigm for understanding whole ecosystem effects of offshore wind farms in shelf seas. *ICES Journal of Marine Science*, 2023. doi: https://doi.org/10.1093/icesjms/fsad194.

Katoh, K., Kume, H., Kuroki, K., and Hasegawa, J. The development of sand waves and the maintenance of navigation channels in the Bisanseto Sea. In *Coastal Engineering 1998*, number 26, pages 3490–3502. ASCE, 1998. June 22-26, 1998. Copenhagen, Denmark.

Knaapen, M. A. F. Sandwave migration predictor based on shape information. *Journal of Geophysical Research: Earth Surface*, 110(F4), 2005. doi: https://doi.org/10.1029/2004JF000195.

Lanckneus, J. and de Moor, G. Present-day evolution of sand waves on a sandy shelf bank. *Oceanologica Acta*, Special Issue 11: 123–127, 1991.

Le Bot, S. and Trentesaux, A. Types of internal structure and external morphology of submarine dunes under the influence of tide- and wind-driven processes (Dover Strait, northern France). *Marine Geology*, 211(1):143–168, 2004. doi: https://doi.org/10.1016/j.margeo.2004.07.002.

Le Bot, S., Bary, M., Fournier, M., Husté, A., Michelet, N., Blanpain, O., Nexer, M., and Garlan, T. Marine dune morphodynamics and sediment fluxes (off Dunkirk, France). Spatio-temporal variability and relations with hydrodynamic forcings. In *Marine and River Dune Dynamics VII Book of Proceedings*, pages 155–162, 2023. April 1-3, 2023. Rennes, France.

Li, X., Chi, L., Chen, X., Ren, Y., and Lehner, S. SAR observation and numerical modeling of tidal current wakes at the East China Sea offshore wind farm. *Journal of Geophysical Research: Oceans*, 119(8):4958–4971, 2014. doi: https://doi.org/10.1002/2014JC009822.

Lokin, L. R., Warmink, J. J., and Hulscher, S. J. M. H. The Effect of Sediment Transport Models on Simulating River Dune Dynamics. *Water Resources Research*, 59(12), 2023. doi: https://doi.org/10.1029/2023WR034607.

Lyard, F. H., Allain, D. J., Cancet, M., Carrère, L., and Picot, N. FES2014 global ocean tide atlas: design and performance. *Ocean Science*, 17(3):615 – 649, 2021. doi: https://doi.org/10.5194/os-17-615-2021.

Margalit, J. *Development of natural seabed forms and their* *interaction with off shore wind farms*. Phd thesis, DTU - Technical University of Denmark, 2017. Retrieved from https://orbit.dtu.dk/en/publications/development-of-natural-seabed-forms-and-their-interaction-with-of.

Melville, B. W. Scour at bridge sites. In *Civil Engineering Practice*, edited by Cheremisinoff, P. N. and Cheremisinoff, N. P., pages 327–362. Technomic Publishing Company, 1988.

Miles, J., Martin, T., and Goddard, L. Current and wave effects around windfarm monopile foundations. *Coastal Engineering*, 121:167–178, 2017. doi: https://doi.org/10.1016/j.coastaleng.2017.01.003.

OpenTopoMap. https://opentopomap.org.

Parc éolien en mer de Dunkerque website. https://parc-eolien-en-mer-de-dunkerque.fr/presentation-du-projet, Last accessed May 10, 2022.

Rivier, A., Bennis, A.-C., Pinon, G., Gross, M., and Magar, V. Regional numerical modelling of offshore monopile wind turbine impacts on hydrodynamics and sediment transport. In *Renewable Energies Offshore*, pages 807–813. CRC Press, 2015. November 24-26, 2014. Lisbon, Portugal.

Rivier, A., Bennis, A.-C., Pinon, G., Magar, V., and Gross, M. Parameterization of wind turbine impacts on hydrodynamics and sediment transport. *Ocean Dynamics*, 66(10):1285–1299, 2016. doi: https://doi.org/10.1007/s10236-016-0983-6.

Schultze, L. K. P., Merckelbach, L. M., Horstmann, J., Raasch, S., and Carpenter, J. R. Increased Mixing and Turbulence in the Wake of Offshore Wind Farm Foundations. *Journal of Geophysical Research: Oceans*, 125(8):e2019JC015858, 2020. doi: https://doi.org/10.1029/2019JC015858.

Shom. MNT bathymétrique de façade Atlantique (Projet HOMONIM). http://dx.doi.org/10.17183/MNT_ATL100m_HOMONIM_WGS84, 2015.

Shom. MNT topo-bathymétrique côtier à 20m du détroit du Pas-de-Calais (Projet TANDEM). http://dx.doi.org/10.17183/MNT_COTIER_DETROIT_PDC_TANDEM_20m_WGS84, 2016.

Shom. 2016 current measurements collected as part of pre-feasibility studies for the Dunkirk offshore wind farm area. https://www.mongeosource.fr/geosource/1111/fre/catalog.search#/metadata/672d497d-65e5-4fba-ac0d-682a85401f19, 2017a.

Shom. 2016-2017 multi-beam bathymetric surveys conducted as part of pre-feasibility studies for the Dunkirk offshore wind farm area. https://www.mongeosource.fr/geosource/1111/fre/catalog.search#/metadata/813b4f9f-80dd-4c77-a66d-4e989be87b72, 2017b.

Shom. 2016-2017 bed samples collected as part of pre-feasibility studies for the Dunkirk offshore wind farm area. https://www.mongeosource.fr/geosource/1111/fre/catalog.search#/metadata/2a0ca78b-514d-425b-beb8-328469fef861, 2017c.

Shom. Sedimentological data produced as part of pre-feasibility studies for the Dunkirk offshore wind farm area. https://www.mongeosource.fr/geosource/1111/fre/catalog.search#/metadata/a23c84cf-5761-4939-8f39-c1e1224097bd, 2017d.

Shom - ROLNHDF. Partie maritime Litto3D® - Normandie et Hauts-De-France 2016-2018. http://dx.doi.org/10.17183/L3D_MAR_NHDF_2016_2018, 2022.

Soulsby, R. L. *Dynamics of marine sands*. Thomas Telford Publishing, 1997. doi: https://doi.org/10.1680/doms.25844.

Stevens, R. J. A. M. and Meneveau, C. Flow Structure and Turbulence in Wind Farms. *Annual Review of Fluid Mechanics*, 49:311–339, 2017. doi: https://doi.org/10.1146/annurev-fluid-010816-060206.

Sumer, B. M. and Fredsøe, J. *The Mechanics of Scour in the Marine Environment*. World Scientific, 2002. doi: https://doi.org/10.1142/4942.

Sutherland, J., Walstra, D.-J. R., Chesher, T. J., van Rijn, L. C., and Southgate, H. N. Evaluation of coastal area modelling systems at an estuary mouth. *Coastal Engineering*, 51(2):119–142, 2004. doi: https://doi.org/10.1016/j.coastaleng.2003.12.003.

Tassi, P., Benson, T., Delinares, M., Fontaine, J., Huybrechts, N., Kopmann, R., Pavan, S., Pham, C.-T., Taccone, F., and Walther, R. GAIA - a unified framework for sediment transport and bed evolution in rivers, coastal seas and transitional waters in the TELEMAC-MASCARET modelling system. *Environmental Modelling & Software*, 159:105544, 2023. doi: https://doi.org/10.1016/j.envsoft.2022.105544.

The Crown Estate. Offshore wind operational report 2020. Technical report, The Crown Estate, 2020.

Tsanis, I. K. Simulation of Wind-Induced Water Currents. *Journal of Hydraulic Engineering*, 115(8):1113–1134, 1989. doi: https://doi.org/10.1061/(ASCE)0733-9429(1989)115:8(1113).

van der Tempel, J., Zaaijer, M. B., and Subroto, H. D. The effects of Scour on the design of Offshore Wind Turbines. In *Proceedings of the 3rd International conference on marine renewable energy (MAREC 2004)*, pages 27–35, 2004. July 7-9, 2004. Blyth, United Kingdom.

van Gerwen, W., Borsje, B. W., Damveld, J., and Hulscher, S. J. M. H. Modelling the effect of suspended load transport and tidal asymmetry on the equilibrium tidal sand wave height. *Coastal engineering*, 136:56–64, 2018. doi: https://doi.org/10.1016/j.coastaleng.2018.01.006.

van Rijn, L. C. Sediment Transport, Part I: Bed Load Transport. *Journal of Hydraulic Engineering*, 110(10):1431–1456, 1984. doi: https://doi.org/10.1061/(ASCE)0733-9429(1984)110:10(1431).

Vanhellemont, Q. and Ruddick, K. Turbid wakes associated with offshore wind turbines observed with Landsat 8. *Remote Sensing of Environment*, 145:105–115, 2014. doi: https://doi.org/10.1016/j.rse.2014.01.009.

VLIZ. Wave data obtained from the Westhinder buoy. https://meetnetvlaamsebanken.be/map, 2022a.

VLIZ. Average wind, air pressure and water level data obtained from the Westhinder measuring platform. https://meetnetvlaamsebanken.be/map, 2022b.

Wang, S.-Y., Qi, W.-G., Li, B., Wang, C., and Gao, F.-P. Tidal currents-induced scour development around pile foundations: Effects of flow velocity hydrograph. *Coastal Engineering*, 191:104533, 2024. doi: https://doi.org/10.1016/j.coastaleng.2024.104533.

Whitehouse, R. J. S. *Scour at marine structures: A manual for practical applications*. Thomas Telford Publishing, 1998. doi: https://doi.org/10.1680/sams.26551.

Whitehouse, R. J. S. and Stroescu, E. I. Scour depth development at piles of different height under the action of cyclic (tidal) flow. *Coastal Engineering*, 179:104225, 2023. doi: https://doi.org/10.1016/j.coastaleng.2022.104225.

Whitehouse, R. J. S., Harris, J. M., Sutherland, J., and Rees, J. The nature of scour development and scour protection at offshore windfarm foundations. *Marine Pollution Bulletin*, 62(1):73–88, 2011. doi: https://doi.org/10.1016/j.marpolbul.2010.09.007.